



HAL
open science

Explaining the groundwater salinity of hard-rock aquifers in semi-arid hinterlands using a multidisciplinary approach

Marjorie Kreis, Jean-Denis Taupin, Nicolas Patris, Virginie Vergnaud-Ayraud, Christian Leduc, Patrick Lachassagne, Julien Burte, Eduardo Martins

► To cite this version:

Marjorie Kreis, Jean-Denis Taupin, Nicolas Patris, Virginie Vergnaud-Ayraud, Christian Leduc, et al.. Explaining the groundwater salinity of hard-rock aquifers in semi-arid hinterlands using a multidisciplinary approach. *Hydrological Sciences Journal*, 2023, pp.1-19. 10.1080/02626667.2023.2253227. hal-04244740

HAL Id: hal-04244740

<https://univ-rennes.hal.science/hal-04244740>

Submitted on 7 Mar 2024

HAL is a multi-disciplinary open access archive for the deposit and dissemination of scientific research documents, whether they are published or not. The documents may come from teaching and research institutions in France or abroad, or from public or private research centers.

L'archive ouverte pluridisciplinaire **HAL**, est destinée au dépôt et à la diffusion de documents scientifiques de niveau recherche, publiés ou non, émanant des établissements d'enseignement et de recherche français ou étrangers, des laboratoires publics ou privés.




Explaining the groundwater salinity of hard-rock aquifers in semi-arid hinterlands using a multidisciplinary approach

Marjorie B. Kreis, Jean-Denis Taupin, Nicolas Patris, Virginie Vergnaud-Ayraud, Christian Leduc, Patrick Lachassagne, Julien D. P. Burte & Eduardo S. P. R. Martins

To cite this article: Marjorie B. Kreis, Jean-Denis Taupin, Nicolas Patris, Virginie Vergnaud-Ayraud, Christian Leduc, Patrick Lachassagne, Julien D. P. Burte & Eduardo S. P. R. Martins (2023): Explaining the groundwater salinity of hard-rock aquifers in semi-arid hinterlands using a multidisciplinary approach, Hydrological Sciences Journal, DOI: [10.1080/02626667.2023.2253227](https://doi.org/10.1080/02626667.2023.2253227)



To link to this article: <https://doi.org/10.1080/02626667.2023.2253227>

 [View supplementary material](#) 

 Accepted author version posted online: 31 Aug 2023.

 [Submit your article to this journal](#) 

 Article views: 22

 [View related articles](#) 

 [View Crossmark data](#) 

Publisher: Taylor & Francis & IAHS

Journal: *Hydrological Sciences Journal*

DOI: 10.1080/02626667.2023.2253227

Explaining the groundwater salinity of hard-rock aquifers in semi-arid hinterlands using a multidisciplinary approach

Marjorie B. Kreis^{a,b,e,*}, Jean-Denis Taupin^a, Nicolas Patris^a, Virginie Vergnaud-Ayraud^c, Christian Leduc^d, Patrick Lachassagne^a, Julien D. P. Burte^d, Eduardo S. P. R. Martins^{b,e}

(a) HSM, Univ Montpellier, CNRS, IRD, IMT Mines Alès, Montpellier, France

(b) Dep. of Civil Engineering, Federal Univ. of Ceará, Fortaleza, Brazil

(c) Univ. Rennes, CNRS, OSUR- Plateforme Condate Eau, Rennes, France

(d) G-EAU, AgroParisTech, CIRAD, IRD, INRAE, Montpellier SupAgro, Montpellier, France

(e) Research Institute of Meteorology and Water Resources (FUNCEME), Fortaleza CE, Brazil

* Corresponding author: marjorie.kreis@hotmail.fr

Abstract

Shallow crystalline groundwater of semi-arid hinterland of Ceará exhibits brackish or saline water with mixed-chloride or sodium-chloride facies. Very few hydrochemical data are available in the area and the drivers behind this salinity are not clearly identified. In this study, an extensive field data collection work was performed to provide new information about the hydrogeological functioning and the salinization processes, through the implementation of piezometric, hydrogeochemical, isotopic (^{18}O , ^2H) and multi-tracer dating (^{14}C , ^3H , CFC, SF_6) monitoring. Piezometric and isotopic data evidence fast flow circulation processes and a high contribution of evaporated surface water to aquifer recharge. Multi-tracer dating shows that groundwater is essentially composed of seasonal vertical infiltration flows that mix with older waters stored in the aquifer. Chemical analyses suggest that groundwater, originally low mineralized, has become progressively saltier due to leaching of salts that were evapoconcentrated either in surface waters or the unsaturated zone during drier periods.

Keywords: hydrogeology; hard-rock aquifers; semi-arid climate; salinization; isotopes; environmental tracers; groundwater dating; hydrochemistry; Brazil

1. Introduction

Groundwater resources in semi-arid and hard-rock areas may be subject to salinity issues that deteriorate water quality for drinking water supply or agricultural activities (Rabemanana et al., 2005; Basavarajappa & Manjunatha, 2015; Sreedevi et al., 2021; Banyikwa, 2023). As a consequence, understanding the processes behind the groundwater salinization is crucial to develop sustainable water resource management. In the semi-arid area of northeastern Brazil (NEB), groundwater from crystalline rocks represents a strategic water resource for the rural populations (MMA, 2007), especially during drought periods. Indeed, this region is frequently affected by intense drought events, and rainfall occurs during a short period of the year with a highly irregular distribution in space and over time (Pontes Filho et al., 2020; Ribeiro Neto et al., 2022). This great climate variability and the consequent vulnerability to drought have led to the construction of a dense network of small and middle/large-sized surface water reservoirs which constitute the

primary source of water supply in the state of Ceará. However, demand pressures added to prolonged droughts boosted the exploitation of the groundwater contained in the crystalline rocks (Da Silva et al., 2007).

The presence of aquifers in hard-rocks is related to the degree of weathering and fracturing of the rock, considering their very low primary porosity and permeability (Wyns et al., 2004; Lachassagne et al., 2011). These chemical and physical weathering processes lead to the in-situ development of saprolite (unconsolidated alterite) and of a subhorizontal permeable fractured layer of several tens of meters thick below the saprolite, due to the stress generated by the swelling of certain minerals such as biotite (Wyns et al., 2004; Lachassagne et al., 2021). The fractured layer is characterized in the first few meters by a dense fracturing decreasing with depth, down to the base of the weathering profile, which results in a decrease in hydraulic conductivity and connectivity between fractures with depth (Lachassagne et al., 2021). Even if plutonic and metamorphic rocks have a low aquifer potential, they represent a valuable water resource in comparison with the scarce surface water. This is why many rural communities in Ceará had no alternative but to drill wells in the crystalline rocks during the last severe drought from 2012 to 2016.

Groundwater from the Ceará crystalline aquifers is characterized by a high and heterogeneous salinity, mostly above the drinking water limit and up to several tens of g.L^{-1} (Burte, 2008; Araújo, 2017). The origin of salinity and the salinization processes of groundwater in semi-arid NEB have been sporadically studied since the 1960s, and the mechanisms behind the groundwater salinity are still debated (Matsui, 1978; Frischkorn & Santiago, 2000; Silva, 2003; Britto Costa et al., 2006; Araújo, 2017). Paradoxically, these waters present short residence times (Salati et al. 1979a; Santiago et al., 2000), implying that the strong salinity observed cannot be explained by a long duration of water/rock interaction. In addition, chloride is often the prevailing anion, which is not consistent with water-rock interactions in crystalline rocks (Shand et al., 2007; Al-

meida et al., 2008). The crystalline aquifers of Ceará have been little studied compared with sedimentary or alluvial aquifers which represent more important water resources in terms of water storage capacity. Consequently, very few data allow characterizing the hydrogeological functioning of such aquifers (Funceme, 2007).

This multidisciplinary study intends to provide new interpretation elements about the Ceará fractured crystalline aquifers through an extensive field data collection work and the simultaneous acquisition of piezometric, hydrochemical, isotopic data and multi-tracer dating (^{18}O , ^2H , ^3H , ^{14}C , CFC, SF_6). Piezometric variations were used to observe the aquifer reactivity and to estimate recharge through the use of the water table fluctuation (WTF) method (Healy & Cook, 2002). Analyses of the water stable isotopes (^{18}O , ^2H) in the different compartments of the water cycle (rain, surface water and groundwater) were performed to identify groundwater recharge processes and the origin and organization of groundwater flows within aquifers (Ahmed et al., 2019; Babaye et al., 2019). Water residence times were determined using ^{14}C and ^3H radioactive tracers, and refined with the first-ever CFC and SF_6 analyses performed in the Ceará state. Water quality data were evaluated using Piper diagram, chemical ratios including the Cl^-/Br^- molar ratio, and principal component analysis (PCA) to identify groundwater facies, the potential sources of ions and the dominant geochemical processes.

The objectives of this study were to (1) assess the hydrodynamics and hydrogeological functioning of the crystalline aquifers, and (2) assess the origin of the groundwater salinity, in order to contribute to the knowledge about groundwater salinity in semi-arid hard-rock areas.

2. Study area

2.1. Geography and land uses

The study area is included in the Banabuiú watershed, whose eponymous river drains from west to east an area of 19647 km². It is located in the centre of the Ceará state, approximately 180 km

from Fortaleza (capital city) and the Atlantic coast (Fig. 1). The hydrogeological investigations were carried out in four sub-basins of the Banabuiú watershed: Forquilha (214 km²), Pirabibú (127 km²), and Vista Alegre (550 km²), all three located in the municipality of Quixeramobim, and Ibicuitinga (286 km²), mainly located in the municipality of Ibicuitinga (Fig. 1). These are rural areas with low human density (about 25 inhab.km⁻²), inserted in the Caatinga biome, whose socioeconomic development is mainly based on livestock (extensive farming) and agriculture (MME, 1998).

2.2. *Climate*

The semi-arid climate has been relatively stable in the study area over the last 13 Ma (Peulvast et al., 2008). It is characterized by a strong water deficit due to a low rainfall regime (< 800 mm.a⁻¹), a high potential evapotranspiration (PET) rate (> 1700 mm.a⁻¹), an irregular rainfall distribution and recurrent drought periods (Martins & Vasconcelos Júnior, 2017; Pontes Filho et al., 2020). The mean annual rainfall is about 700 ± 275 mm in the study area (1912-2021 period) with minimum and maximum values of 154 and 1441 mm respectively. The wet season extends from December to July and 75 % of the annual precipitation falls between February and May. The four rainiest months, locally called "quadra-chuvosa", result from the movement of the Intertropical Convergence Zone (ITCZ), which is formed by the confluence of the northeast and southeast trade winds, and is characterized by strong upward air movements and heavy rains in the north of the NEB (Da Silva et al., 2017). Consequently, the rain generally falls intensely in the region during this period.

The monthly PET is always higher than the monthly precipitation, except in March and April (Supplementary material Figure S1). As a result, these two months are theoretically the most likely to produce the annual runoff and groundwater recharge. However, the amount of rainfall contributing to runoff or recharge cannot be directly deduced from a monthly water balance in such a climatic context; taking into account the daily scale is required. The region regu-

larly suffers from droughts lasting several years. During the last prolonged drought (2012-2019), the 2012-2016 period was the most severe 5-year drought ever recorded in the area (40 % decrease in annual rainfall). The average annual temperature is 27.2 °C, with monthly mean extrema of 25.7 °C and 28.5 °C (Supplementary material Figure S1). Monthly relative humidity varies between 41.6 % (July) and 85.9 % (February), with an annual average of 61.0 %.

2.3. *Geology and geomorphology*

The crystalline rocks constitute 96.5 % of the Banabuiú watershed area. They consist of various types of Precambrian gneisses and migmatites (3.2 Ga to 541 Ma), associated with plutonic and metaplutonic rocks of predominantly granitic composition (INESP, 2009). The different lithostratigraphic units have a NE-SW orientation (Supplementary material Figure S2). The remaining 3.5% are composed of Tertiary-Quaternary sediments that appear in scattered patches and are interpreted as fluvial-lacustrine deposits (Da Silva et al., 2003), but also of alluvial and colluvial-eluvial Quaternary sediments deposited along watercourses in low-slope areas.

Elevation of the Banabuiú watershed ranges from 1154 m asl (West) to 30 m asl (East). The landscape is dominated by hinterland depressions (78 % of the basin area, called Sertaneja Depression and represented by a flat and slightly undulating relief. The Sertaneja Depression was formed from a large pediplanation process that produced the current surface of the Precambrian rocks, corresponding to the lower parts of the basin (< 300 - 400 m asl). In opposition, elevations above 300 - 400 m asl correspond to the reliefs formed by the residual massifs (inselbergs, mountains or plateaus), evidence of the action of weathering and erosion over millions of years.

2.4. *Hydrological and hydrogeological setting*

In the crystalline zones of the study area, surface runoff is of Hortonian type due to the low thickness (<1 m) and the low permeability of soils (Burte, 2008). All rivers in Ceará are naturally

intermittent (Santiago et al., 2001). Nascimento (2016) estimated that 90 % of the surface water flows during the “quadra-chuvosa”, between February and May, although with a great interannual variability. River discharge is generally intense, short and irregular (Burte, 2008). River recession time is short (Santiago et al., 2001). The intermittence of water courses and the recurrence of drought pressed public policy makers to promote the construction of dams to guarantee the water supply during the periods of water stress (Santiago et al., 2001; Burte, 2008). As a result, the Banabuiú watershed hosts numerous dams, with 17299 reservoirs over 20 m in length being registered by the FUNCEME (Freitas Filho & Carvalho, 2021). Among them, 1415 reservoirs have an area greater than 5 ha (INESP, 2009). In addition to these dams, temporary ponds of various size form in the topographic lowlands when it rains (Araújo, 2017). These reservoirs are subject to high evaporation rates and, consequently, to significant issues of salinization and eutrophication.

In the semi-arid NEB, the saprolite is generally thin or non-existent (MMA, 2007) because of erosion. This allows a direct connection between the surface drainage system and the fractured layer. In the study area, the median thickness of the saprolite layer is about 9 ± 6 m, while the underlying fractured layer is about 50 meter thick (Kreis, 2021). In the Ceará State, the median depth of boreholes is about 60 m and the piezometric level is generally met at a depth of 10 m (Da Silva et al. 2007), which implies that groundwater is mainly present in the fractured layer. The boreholes in the crystalline aquifers in NEB are characterized by low discharges (< 1 to $3 \text{ m}^3 \text{ h}^{-1}$) and specific capacities of less than $1 \text{ m}^3 \text{ h}^{-1} \text{ m}^{-1}$ (Asomaning, 1992; MMA, 2007; Feitosa, 2008). Transmissivity is low, between 1.10^{-6} and $7.10^{-5} \text{ m}^2 \text{ s}^{-1}$ (Manoel Filho, 1996). As in most crystalline aquifers (Lachassagne et al., 2021), there is no regional flow (Santiago et al. 2000), which means that the natural outflow from these aquifers feeds the rivers or alluvial aquifers, at the scale of small local sub-basins, when evapotranspiration does not recover all flows (Burte, 2008). In Ceará, in addition to these groundwater flows from crystalline aquifers to the

alluvial ones, recharge of alluvial aquifers mostly comes from diffuse infiltration of rainfall and localized infiltration from the rivers (Funceme, 2007). The reversal of flow between the rivers and the alluvial aquifers, which prolongs their flow, can be observed locally at the end of the rainy season (Funceme, 2007).

3. Materials and methods

The comprehension and characterization of the hydrogeological and hydrochemical functioning of complex hydrosystems require a multidisciplinary approach. Each method only provides clues that, when they converge, combine to efficiently deepen the knowledge of the system (e.g. Marchal et al., 2014). For this study, investigations were developed along two main axes. On one hand, the study of subterranean hydrodynamics based on the implementation of a piezometric monitoring network and the realization of a multi-tracer sampling program (^{18}O , ^2H , ^3H , ^{14}C , CFC, SF_6). On the other hand, the study of the hydrochemical composition and evolution of the groundwater through an electrical conductivity (EC) monitoring and the analysis of major, minor and trace ions. Results of the first axis allow to characterize groundwater recharge, circulation processes and water residence times, while results of the second axis provide information about the types of salts involved and their evolution over time. All these elements give insights into the processes that lead to groundwater salinization and salinity dynamics.

3.1. Characterization and quantification of aquifer recharge from piezometric monitoring

Monthly and hourly piezometric data were collected respectively from March 2018 to December 2019 over a network of 56 boreholes (monthly monitoring), and from November 2016 to December 2019 in four of these boreholes (hourly monitoring). Existing piezometric data were also exploited, including 93 measurements generally taken quarterly (monthly for the borehole FOR-Y22) between 2010 and 2016 in seven of the boreholes used in the 2018-2019 monthly monitor-

ing, and 73 sporadic piezometric measurement carried out between August 2016 and March 2018 in the 56 boreholes of the monthly monitoring. Monthly piezometric measurements were taken manually, while hourly piezometric measurements were performed with Rugged TROLL[®]100 pressure sensors (absolute pressure measurement) and a Rugged TROLL[®] barometer, branded Aquatroll from In-situ Inc. The pressure measurement accuracy is ± 0.1 % of the full scale (± 3 cm). The monitored boreholes are located in Fig. 1.

Piezometric data were collected to characterize the reactivity of the aquifer in response to rainfall and to estimate the aquifer recharge through the use of the WTF method. The WTF method was applied as an exploratory approach. It requires that the specific yield is known and that the piezometric level rise is only due to the vertical infiltration of the recharge through the unsaturated zone (USZ). The recharge rate can be inferred from the seasonal water fluctuation:

$$R = (\Delta WL / \Delta t) \times S_y \quad (1)$$

where R is the recharge rate, ΔWL the variation of the piezometric level, Δt the time period and S_y the specific yield (Healy and Cook, 2002). In the absence of any direct measurement of S_y in the study area, we used values from the literature, as discussed later.

3.2. Characterization of recharge processes and surface-groundwater relationships from water stable isotopes (¹⁸O, ²H)

Stable isotopes ($\delta^{18}\text{O}$, $\delta^2\text{H}$) analyses were performed on:

- Rainwater, sampled monthly between January and July (the period concentrating 95 % of the annual precipitation) from 2011 to 2019 in three rainfall stations (Inmet-Quixeramobim, Algodões-Zé Nobre and Vista Alegre; 172 samples), and at a daily frequency between March 2018 and December 2019 in two rainfall stations (Radar and Riacho Verde; 212 samples).

- Groundwater, sampled from a network of 75 borewells (137 samples), one well (2 samples) and one spring (2 samples), all from the crystalline aquifers during different hydrological periods between August 2016 and August 2019. Historical stable isotope data (Burte, personal communication) generally taken quarterly from 12 boreholes (62 samples) between August 2009 and December 2012 to observe seasonal variations, and from 2 wells (2 samples), were also added to the database.
- Surface water, collected in 3 different reservoirs in 2009 (3 samples) and 2018 (3 samples). Historical data, taken quarterly in 7 different reservoirs of the study region in 2012 (59 samples) by Rebouças and Taupin (personal communication), were also used.

The location of the rain gauges is given in Supplementary material (Table S1) and the location of the sampled borewells and wells is plotted in Fig. 2. Groundwater samples were collected after a 30 min pumping or after the stabilization of the physicochemical parameters (pH, temperature and EC) to ensure a good representativeness. Daily precipitation of less than 1 mm day⁻¹ was not sampled. All samples were packaged in 20 mL transparent plastic bottles, hermetically closed by an inner cap and a plastic lid, and stored in a dark refrigerated container. Analyses were performed at the HydroSciences Montpellier (HSM, France) water stable isotope laboratory (LAMA). Results are given in delta permil units (δ , ‰) vs V-SMOW, with an analytical error of ± 0.08 ‰ for $\delta^{18}\text{O}$ and ± 0.8 ‰ for $\delta^2\text{H}$.

3.3. *Groundwater multi-tracer dating (^{14}C , ^3H , CFC and SF_6)*

Groundwater residence times were obtained from the sampling of 3 borewells in November 2009 and 7 borewells in February 2018 for ^{14}C and ^3H analyses. The ^{14}C analyses were completed with $\delta^{13}\text{C}$ analysis to model the water's radiocarbon apparent age by differentiating the biogenic source of carbon. This dating was complemented by CFC and SF_6 analyses collected from 10 borewells in June 2019, whose results correspond to the first CFC and SF_6 measurements ever

carried out in Ceará. Unfortunately 5 boreholes sampled for ^{14}C and ^3H measurements were no longer available to be sampled again for the CFC and SF_6 analysis in 2019; they were replaced by other boreholes. The groundwater $\delta^{13}\text{C}$, ^{14}C and ^3H analyses were carried out at the Avignon University (France) EMMAH laboratory. The ^{14}C results are expressed in percent of modern carbon (pMC), with pMC = 100 % corresponding to post-1950s infiltrated waters. The analytical error is about 0.5 pMC. The $\delta^{13}\text{C}$ results are expressed in delta permil units (δ , ‰) vs V-PDB, with an analytical error of ± 0.1 ‰. The ^3H results are expressed in tritium units (TU), with an analytical error which varies from 0.3 to 0.6 TU. Analyses of CFC11, CFC12, CFC113 and SF_6 water concentrations were performed at the Condade Eau - OSUR analytical platform of the University of Rennes (France). Analyses are within 3 % accuracy for CFCs, and within 5 % for SF_6 . The location of the sampled borewells is given in Fig. 2.

3.4. Hydrochemical analyses (EC, major ions, minor ions and trace elements)

An EC monitoring was conducted simultaneously with the monthly piezometric monitoring to evaluate the dynamics of groundwater salinity over time. Major ions (Ca^{2+} , Mg^{2+} , Na^+ , K^+ , HCO_3^- , CO_3^{2-} , Cl^- , SO_4^{2-} , NO_3^- , NO_2^-) sampling campaigns were carried out in December 2017 (end of the dry season) and June 2018 (end of the wet season) in 27 and 38 borewells, respectively. Major ion analyses were performed at the Ceará Water and Sewerage Company (CAGECE) (Fortaleza, Brazil) GECOQ laboratory, in accordance with methodologies recommended by APHA (2012). To improve the understanding of the geochemical sources at the origin of the groundwater salinity, a sampling campaign for major ions (Ca^{2+} , Mg^{2+} , Na^+ , K^+ , Cl^-), minor ions (Br^-), and trace elements (Li, B, Al, Si, P, S, Ti, V, Cr, Mn, Fe, Co, Ni, Cu, Zn, Ga, As, Se, Rb, Sr, Y, Mo, Ag, Cd, Sn, Sb, Cs, Ba, La, Ce, Pr, Nd, Sm, Eu, Tb, Gd, Dy, Ho, Er, Tm, Yb, Lu, Tl, Pb, Th, U) was implemented on 20 borewells in June 2019. Samples were analysed at the HSM AETE-ISO platform (Montpellier, France).

The Piper diagram was used to determine the hydrogeochemical facies and the effects of the seasonal recharge on the ionic composition, while the ionic ratios (binary plot investigations) were calculated to identify potential sources of salts. Cl^-/Br^- molar ratio was used as an indicator of the source of the chloride ion (Cartwright et al., 2006; Alcalá & Custodio, 2008). The PCA method was used on chemical data to strengthen the identification of the processes controlling groundwater chemistry. PCA statistically quantifies the relationship between variables and the contribution and significance of each variable. It is a multivariate statistical analysis method that transforms correlated variables into uncorrelated principal components (PC) that represent the directions of maximum variance in the data. The projection of the PC on factorial axes allows for the identification of patterns and relationships between the variables by defining which variables contribute the most to the variance in the data. The interest of this technique is to summarize the maximum amount of information contained in the mass of data on such factorial axes.

4. Results and interpretation

4.1. Evolution of piezometric levels and recharge rate assessment

Piezometric levels in the crystalline aquifers are relatively shallow, between 0.4 and 21.4 m below the ground surface, with a mean value of around 10 m. Their contrasted temporal variations confirm that there is no regional flow. The severe 5-year drought of 2012-2016, marked with a 40 % decrease in the annual rainfall, caused a general lowering of the piezometric level, up to 7 m (Fig. 3). Even during these dry years, the monthly monitoring of the borewell FOR-Y22 highlighted a recharge of the crystalline aquifer, except in 2016. The rainier conditions between 2017 and 2019 (annual rainfall only 10 % below the 1912-2021 average) allowed to reconstitute the water stock. This underlines the dependence of recharge on climatic fluctuations, which is common in such low specific yield aquifers (Dewandel et al., 2010).

Generally, the seasonal recharge of the crystalline aquifers occurs between February and May ("quadra-chuvosa" period), and mostly in March and April. The hourly monitoring carried out between November 2016 and December 2019 (Fig. 4) highlighted that recharge does not directly depend on the annual or monthly rainfall amounts. Moreover, a gradual increase of the groundwater level is observed throughout the rainy season (Fig. 4), even if a strong reaction of the piezometric level is observed in less than 24 h after significant rain events (> 50-60 mm). However, a decrease in the piezometric level is almost never observed following such events during the rainy season. The seasonal recharge depends on the distribution and quantity of daily rainfall and is favoured by the storage of surface runoff in ponds, as observed in other semi-arid areas (Leduc et al., 1998). During the dry period, water levels decrease due to the absence of recharge while the aquifer discharge continues through the river baseflow or evapotranspiration processes.

4.2. Assessment of aquifer recharge rates

In semi-arid areas, the determination of the amount of recharge using conventional water balance and/or hydraulic methods is tricky (Ahmed et al., 2019). Moreover, the use of the monthly scale for water balance calculations is not adapted to semi-arid regions with highly variable and often intense rainfall events. Thus, water balance calculations based on monthly data, as attempted by Araújo (2017) for example (yielding maximum recharge rates of 12 % of the annual rainfall), are not realistic. Furthermore, a maximum soil retention capacity of 100 mm is generally used for this type of calculation, and this value is likely to be overestimated: aquifer recharge can occur with a monthly rainfall of about 60 mm, as observed for instance in the PIR-P14 borehole in January 2018 (Fig. 4). In this study, recharge rate estimates were then approached using the WTF method and based on a multi-event time series analysis (Healy & Cook, 2002; Crosbie et al., 2005; Maréchal et al., 2006). It was used here only as an exploratory approach, considering that the specific yield data are based on the bibliography and that the hourly piezometric moni-

toring suggests the influence of a sub-horizontal flow coming from localized infiltration zones such as ponds and reservoirs. The assessment of the aquifer recharge was performed from the hourly piezometric monitoring of the boreholes PIR-P14 and IBI-P24. Only the rainfall that fell during the period when the piezometric level rose was considered. Manoel Filho (1996) is the only author who provided estimates of the specific yield in Ceará, from 24 boreholes, with values varying from 0.0022 % to 0.28 %. Unfortunately, the S_y values were calculated from single well production tests, without any distant piezometer, which makes these results unrepresentative. The choice of 0.3 % for S_y was based on the existing literature about the fractured layer in similar crystalline aquifers from other regions of the world (Dewandel et al., 2010; Mizan et al., 2019) and in coherence with the recharge rate determined with the ^3H tracer (Kreis, 2021). With a specific yield of 0.3 %, the recharge of the crystalline aquifer is around 1 to 3 % of the annual rainfall (i.e. around 8 to 22 mm a⁻¹), as detailed in Supplementary material Table S2. These results are consistent with those from other semi-arid regions of the world: for Scanlon et al. (2006) in their synthesis of about 140 sites in all continents, the average recharge was between 0.1 and 5 % of the long-term average annual precipitation.

4.3. Recharge processes and surface-groundwater relationships inferred from the isotopic composition (^{18}O , ^2H) of rainfall, groundwater and surface water

The daily monitoring of rainwater between 2018 and 2019 showed $\delta^{18}\text{O}$ values ranging from -12.97 ‰ to +2.27 ‰, $\delta^2\text{H}$ values ranging from -98.5 ‰ to +20.2 ‰, and evidenced a high variability of the isotopic composition of rainfall, typical of dry tropical regions with strong seasonal contrasts (e.g. Taupin et al., 1997). The annual amount-weighted mean isotopic composition of rainfall calculated from this dataset is -3.21 ‰ for $\delta^{18}\text{O}$ and -12.0 ‰ for $\delta^2\text{H}$ (n = 212). Only 9 % of the daily rainwater samples showed marked evaporated values with deuterium-excess (d-exc) lower than +8.5 ‰. Conversely, rainwater samples of the monthly monitoring over the 2011-2019 period revealed highly evaporated values. Indeed, 33 % of the monthly data showed d-exc

values $< +8.5$ ‰ regardless of the amount of rainfall. Moreover, the $\delta^{18}\text{O}$ vs $\delta^2\text{H}$ plot evidenced that the monthly samples ($n = 172$) align along an evaporated isotopic line with a slope of 6.41 ($r^2 = 0.90$). The comparison of the monthly samples $\delta^{18}\text{O}$ values with the monthly isotopic signal calculated from amount-weighted daily $\delta^{18}\text{O}$ during the same period (2018-2019) and between two stations with similar environmental characteristics highlighted that the monthly data suffered from an isotopic bias probably due to the partial evaporation of the water stored in the water collector during the monthly storage. Nonetheless, the main features and relative variations of the monthly monitoring are consistent with those of the daily monitoring, and highlight the seasonal variability of the isotopic composition of precipitation at the monthly scale. Indeed, the monthly isotopic concentrations obtained from the daily amount-weighted $\delta^{18}\text{O}$ are most depleted during the main rainy season (from February to May), particularly between March and April when $\delta^{18}\text{O}$ values can decrease from -3.09 ‰ to -5.08 ‰ (Supplementary material Figure S3). These seasonal variations are consistent with those observed in Fortaleza (Da Silva Nobre et al., 2019).

The monitoring of the groundwater isotopic composition, based on 205 samples originating from 78 distinct borewells sampled between 2009 and 2018, showed a wide range of values varying from -4.19 to $+1.76$ ‰ for $\delta^{18}\text{O}$, -25.1 to $+8.0$ ‰ for $\delta^2\text{H}$, and from -8.6 to $+11.6$ ‰ for d-exc. Moreover, historical isotopic data obtained from the 2009-2012 quarterly monitoring showed a seasonal variation of the groundwater $\delta^{18}\text{O}$ composition, which ranged from -3.90 ‰ to -1.03 ‰ over the borewells. The observation of a high spatio-temporal variability of the groundwater isotopic signal, even between two neighbouring borewells, confirms the strong lateral compartmentalization of the aquifers implying that vertical transfers prevail over horizontal transfers, consistently with the literature about crystalline aquifers (Guihéneuf et al., 2014; Alazard et al., 2016; Lachassagne et al., 2021). It also reveals the occurrence of local recharge processes displaying the spatial variability of localized infiltration). Moreover, the seasonal vari-

ation of the groundwater $\delta^{18}\text{O}$ implies rapid recharge and circulation processes within the aquifer.

Water isotopic compositions of the non-evaporated rainfall samples (i.e. with d-exc values $\geq +8.5$ ‰) were plotted to determine the Local Meteoric Water Line (LMWL; Fig. 5). The groundwater and surface water samples were also plotted, which allows to better understand the water's origin and the recharge processes (Fig. 5). The LMWL of Quixeramobim obtained from the monthly and daily rainfall datasets is defined by the equations Eq.2 and Eq.3, respectively:

$$\delta^2\text{H} (\text{‰}) = 7.81 \times \delta^{18}\text{O} (\text{‰}) + 11.3 \text{ ‰} \quad (r^2 = 96 \text{ \%}; n = 115) \quad (2)$$

$$\delta^2\text{H} (\text{‰}) = 8.09 \times \delta^{18}\text{O} (\text{‰}) + 14.1 \text{ ‰} \quad (r^2 = 98 \text{ \%}; n = 192) \quad (3)$$

Slopes of Eq.2 and Eq.3 are close to that of the Global Meteoric Water Line (GMWL), but their y-intercept value is greater (+11.3 ‰ and +14.1 ‰ vs +10.0 ‰) despite the proximity of the study area to the Atlantic coast, considered as the dominant source of moisture. The non-evaporated precipitation record obtained from the study region in Moura (2013) or from Fortaleza in the IAEA-GNIP available data also evidence a y-intercept value higher than 10 ‰, being of +11.4 ‰ ($r^2 = 98 \text{ \%}$, $n = 12$, 2011-2012 period) and +11.6 ‰ ($r^2 = 96 \text{ \%}$, $n = 68$, 1965-1984 period), respectively. The high y-intercept value of Quixeramobim traces the mixing in rainwater of moisture from marine origin and continental recycling (Salati et al., 1979b).

Groundwater and surface water data are distributed along linear regression lines (Fig. 5) which are defined by Eq.4 and Eq.5, respectively:

$$\delta^2\text{H} (\text{‰}) = 5.00 \times \delta^{18}\text{O} (\text{‰}) - 2.1 \text{ ‰} \quad (r^2 = 89 \text{ \%}; n = 205) \quad (4)$$

$$\delta^2\text{H} (\text{‰}) = 4.92 \times \delta^{18}\text{O} (\text{‰}) - 2.3 \text{ ‰} \quad (r^2 = 98 \text{ \%}; n = 65) \quad (5)$$

The $\delta^{18}\text{O}$ values from surface water, varying between -1.32 ‰ and +9.23 ‰, and the slope of 4.92 (Eq.5), clearly indicate that surface water was affected by evaporation. In addition, Eq.5 is similar to the linear regressions obtained by Matsui (1978) and Stolf (1977) for surface

waters reservoirs in the NEB, which are $\delta^2\text{H} = 4.6 \times \delta^{18}\text{O} - 0.5$ ($r^2 = 0.97$, $n = 67$) and $\delta^2\text{H} = 4.75 \times \delta^{18}\text{O} - 1.3$, respectively. Thus, Eq.5 symbolizes the regional evaporation line.

Groundwater data points are scattered between the isotopic poles of rainwater and surface water (Fig. 5), suggesting the contribution of both poles to the recharge processes. Moreover, the slope of Eq.4 and the d-exc values of groundwater clearly show that meteoric waters undergo significant evaporation before their infiltration into aquifers. Thus, the substantial similarity between Eq.4 and Eq.5 highlights that groundwater recharge is not only constituted by the diffuse infiltration of rainwater, but also and mainly by localized infiltration of evaporated surface water. This hypothesis was confirmed by the piezometric survey and is consistent with the presence of numerous reservoirs, ponds and temporary drainage networks in the study area.

The intercept between the linear regressions of groundwater and rainfall (Fig. 5) shows an offset of about -2 ‰ in $\delta^{18}\text{O}$ compared to the annual amount-weighted mean isotopic composition of rainfall, which typically represents the isotopic input signal for groundwater. However in this case, the offset might be due to the natural inter-annual variability of the rainfall isotopic composition or may indicate that most aquifer recharge occurs during the intense rainfall events of the rainy season, particularly in March and April. This last hypothesis is consistent with the piezometric monitoring, and with similar research (e.g. Blavoux et al., 2013 who used another tracer: tritium).

The $\delta^{18}\text{O}$ values of rainwater and surface water were used to infer the fraction of water that infiltrates indirectly in the aquifer. A $\delta^{18}\text{O}$ value of -5‰ was assigned to rainwater, as it is considered that the aquifer recharge occurs mainly during the wettest month of the rainy season. Concerning the isotopic value of surface water, most of the samples were collected from large reservoirs that do not dry up during the year and that, consequently, present more enriched $\delta^{18}\text{O}$ values ($+1.78\text{‰} < \delta^{18}\text{O} < +9.23\text{‰}$). However, small reservoirs ($-1.32\text{‰} < \delta^{18}\text{O} < +1.65\text{‰}$) are more prevalent in the region (Molle and Cadier, 1992), and are probably more propitious to lose

water through leakage due to the absence of a rigorous building method. Therefore, it was estimated that the isotopic signal of surface water undergoing infiltration may vary between -1 and +1‰. From these assumptions, it is estimated that for 67 to 32% of wells, the fraction of evaporated water in the recharge is greater than 50%, and that the mean localized recharge rate varies from 65 to 44% of the total recharge, depending on the assumptions made about the isotopic value of surface water.

4.4. Groundwater residence time determination

A multi-tracer approach based on the ^{14}C , ^3H , CFC and SF_6 contents in groundwater was implemented. Carbon-14 and tritium values ranged from 73.2 to 126.7 pMC and from ≤ 0.3 to 1 TU, respectively (Supplementary material Table S3). Carbon-13 delta values varied from -17.84 ‰ to -14.02 ‰, corresponding to the expected range of carbon-13 values produced by the respiration of C3 plants, which means that no geological or sedimentary input of carbon may disturb the apparent ages that can be directly calculated from the radioactive decay law (Supplementary material Table S3). Thus, ^{14}C values generally higher than 100 pMC and measurable values of ^3H indicate that the waters recharging aquifers were mainly infiltrated after the 1950s nuclear tests.

However, the flow path organization within fractured crystalline aquifers is complex. The CFC and SF_6 data presented in the Supplementary material Table S4 and best interpreted by a binary mixing model (BMM) underline this complexity. The results show the mixing of two types of water, including a recent pole (15 to 85 % contribution) corresponding to the present-day recharge, and an older pole infiltrated before the 1960s. Consequently, the apparent age of groundwater varies from a few decades to hundreds of years albeit with a significant contribution of post-1950s water. This implies fast flow processes, except in a few particular cases. The strong contribution of a current recharge validates the hypothesis of rapid recharge and vertical circulation processes observed with the water stable isotope data, superimposed on a scarcely circulating stock of old water (Kreis et al., 2020). The presence of older waters is a common

finding in crystalline aquifers, as their deepest fractures are poorly connected to the more superficial ones (Guihéneuf et al., 2014; Alazard et al., 2016 Lachassagne et al., 2021).

4.5. Hydrochemical characterization of groundwater

4.5.1 Electrical conductivity (EC)

The EC values of the crystalline groundwater measured between 2016 and 2019 on 56 distinct borewells ranged from 886 to 19310 $\mu\text{S cm}^{-1}$, with a median value of 2854 $\mu\text{S cm}^{-1}$. The mean value and standard deviation were 3561 and 3064 $\mu\text{S cm}^{-1}$, respectively. The large range of variation, the high standard deviation and the salinity differences observed between neighbouring wells confirm the strong spatial heterogeneity in the crystalline aquifer, already demonstrated in this paper. Moreover, a strong vertical stratification was also observed in 15 borewells, with EC increasing with the depth within the fractured layer (Kreis, 2021). The absence of a salinity gradient at the sub-basin scale, associated with the absence of regional flow as demonstrated notably by piezometric data, implies that the observed salinity differences between the borewells are linked to local environmental processes. No relationship was found between the apparent age, or the stable isotopic composition, and the EC of the groundwater. However, the rainy season generally induces an increase in EC within the borewells (Supplementary material Figure S4), which may be caused either by evapoconcentration of dissolved species in the surface water bodies before infiltration, a leaching of salts stored in the USZ, or the increase of an upwards vertical flow component due to higher piezometric heads.

4.5.2 Major ions

The whole set of 65 analyses from 41 active borewells had an ionic balance error of less than 10 %, therefore all results were used for chemical interpretation. This 10 % limit is higher than the traditionally accepted standard (5 %), but allowed to significantly expand the number of borewells used for the chemical study. Furthermore, 62 % of these analyses showed an ionic

error of less than 5 %, and 85 % had an imbalance < 7 %. All analyses with an ionic error between 5 % and 10 % had a dominant cation or anion exceeding 40 % of the total cation or anion content. Thus, the 10 % bias does not really affect the determination of the chemical facies. Therefore, setting the ionic balance acceptance limit at 10 % did not introduce significant biases in the interpretation of the chemical facies or geochemical processes at the origin of salinization (Zakaria et al., 2015). Groundwaters are characterized by high concentrations in chloride and sodium. Chloride concentrations varied from 29 to 5126 mg L⁻¹, with a median value of 702 mg L⁻¹, while sodium concentrations ranged from 98 to 1800 mg L⁻¹, with a median value of 275 mg L⁻¹ (Table 1). An excellent correlation is observed between the EC values and the chloride concentration ($r^2 = 0.96$), which indicates that the salinity (represented here by EC) derives essentially from chloride salts and, to a lesser extent, calcium ($r^2 = 0.79$), magnesium ($r^2 = 0.69$), and sodium ($r^2 = 0.68$). No relationship is observed between EC and bicarbonate, sulphate or nitrate ($r^2 < 0.1$). The chemical analyses highlighted that 49, 22, 11, 5 and 4 % of the samples present a Na-Mg-Cl, Na-Cl, Na-Mg-Cl-HCO₃, Mg-Cl or Na-Cl-HCO₃ facies, respectively (Fig. 6). Nevertheless, Na-Mg-HCO₃ and Na-HCO₃ facies are observed for the less salty waters (with EC < 1600 $\mu\text{S cm}^{-1}$). Results show that the proportion of chloride increases with the salinity and exceeds that of bicarbonate until reaching percentage levels up to 50 % of the total ionic content for the most saline waters (Supplementary material Figure S5).

Groundwater samples collected before (December 2017) and after (June 2018) the rainy season are plotted on Piper diagrams (Fig. 6). The rainy season generally caused a shift of the points in the cation sector from the sodium pole, dominant at the end of the dry season, towards the mixed area (Fig. 6). This observation suggests, in association with the observed increase in salinity, that processes such as calcium and/or magnesium salts dissolution (as calcite, dolomite or even magnesium-chloride salts) may be involved. For the anions, the evolution of the groundwater chemical composition during the different hydrological periods is more complex,

with distinct behaviours according to the wells especially in terms of chloride and bicarbonate proportions. Nonetheless, an increase in chloride ions is generally observed at the end of the rainy season compared to bicarbonates (in coherence with the EC increase). This increase is not necessarily linked with an increase in nitrate or sulphate concentrations, and suggests therefore that the seasonal increase in salinity is not associated with the recharge of contaminated water (from agriculture and/or waste water), but, as already stated, with the mobilization of more mineralized, possibly older waters.

Nitrate does not show a significant correlation with the other chemical elements. However, groundwaters show high nitrate concentrations with median and maximum values of 71 and 690 mg L⁻¹, respectively. The highest values of nitrate observed are explained by livestock farming as well as evapoconcentration. Indeed, in the study area, all the borewells with nitrate concentrations over 50 mg.L⁻¹ are localized near agricultural or residential areas. Thus, nitrate in groundwater may result from the use of organic fertilizers (KNO₃) and manure, fecal contamination from animals, lack of wastewater treatment or poor septic systems, or even from the decomposition of plant and animal matter. Natural sources may also contribute to high nitrate concentrations, through the presence of termite mounds or nitrogen-fixing trees such as acacias (Schwiede et al., 2005) in the study area. More investigations (with δ¹⁵N, for example) should be carried out to evaluate the main sources of the nitrate. The absence of correlation between nitrate and chloride concentrations confirms that salinity is not directly linked to anthropic pollution, even if human activities can contribute as an additional source of salts.

4.5.3 Minor ions and trace elements

Minor ions and trace elements were determined from a set of 20 borewells, whose electrical conductivity varied from 975 to 15780 μS cm⁻¹ with a median value of 2392 μS cm⁻¹. These samples are characterized by a median concentration of silica (Si⁴⁺) of 45 mg L⁻¹, and a relatively limited

range of values between 28 and 62 mg L⁻¹ (Supplementary material Table S5). Bromide (Br⁻) concentrations ranged from 0.2 to 16 mg L⁻¹, with a median value of 1.0 mg L⁻¹. Regarding trace elements, groundwaters are mainly characterized by the presence of strontium, barium, boron and phosphorus, with median concentrations of 977, 514, 142 and 131 µg L⁻¹, respectively. Standard deviations are high (Supplementary material Table S5) and large differences in concentration can be observed, even between neighbouring borewells, which reflects the strong spatial variability of the aquifers lithology.

The Si⁴⁺ present in most waters derives from aluminosilicate minerals such as feldspars and ferromagnesium silicates (Shand et al., 2007). Si⁴⁺ values measured in this work are slightly higher than the concentrations usually found, and are suggestive of water-rock interaction processes leading to mineral hydrolysis (e.g. Pradeep et al., 2016; Marçais et al., 2018 or N'guettia et al., 2019). Water evapotranspiration processes could explain the high Si⁴⁺ values. In any case, there is no relationship between EC and Si⁴⁺, even for the least salty waters. Conversely, Br⁻ does not derive from the hydrolysis of silicate mineral (Kloppmann et al., 2011), and an excellent correlation between bromide and chloride ($r^2 = 0.99$) was observed. The groundwater Cl⁻/Br⁻ molar ratios ranged from 255 to 1217 (Supplementary material Table S6), with a mean Cl⁻/Br⁻ molar ratio of 815 ± 198 . All the samples with a concentration of chloride above 100 mg L⁻¹ presented a Cl⁻/Br⁻ ratio similar to or higher than the oceanic ratio of ~ 650 (Drever, 1997). On the other hand, the P17 borewell which has the lowest salinity and a chloride content of around 20 mg L⁻¹ showed a much lower Cl⁻/Br⁻ ratio (~ 255). Thus, the Cl⁻/Br⁻ molar ratio in the P17 borewell could be interpreted as reflecting that of the local rainfall (Cartwright et al., 2006). The increase of the Cl⁻/Br⁻ molar ratio in the other borewells, associated with an increase of Cl concentration, is suggestive of halite dissolution during recharge (Cartwright et al., 2006; Alcalá & Custodio, 2008). The fact that Cl⁻/Br⁻ ratios remain relatively constant as Cl concentrations increase above 300 mg L⁻¹ provides evidence that another factor responsible for the rise in groundwater salinity

may be evapotranspiration (Cartwright et al., 2006; Alcalá & Custodio, 2008). Investigation with $\delta^{37}\text{Cl}$ or ^{36}Cl could be useful to determine the origin of chloride or to constrain processes (e.g. evapotranspiration) affecting groundwater (Cartwright et al., 2006; Kloppmann et al., 2011).

Strontium, barium, boron and phosphorus are traditionally found in silicate and carbonate minerals. Ba^{2+} and Sr^{2+} values in groundwaters are generally of the order of hundreds of $\mu\text{g L}^{-1}$ (Blum et al., 2001; Shand et al., 2007) as is the case in our study. Strontium can also derive from the dissolution of evaporite minerals, and in that case may reach concentrations of the order of tens of mg L^{-1} . In crystalline regions, boron concentrations generally do not exceed a few $\mu\text{g L}^{-1}$ (Blum et al., 2001), but it may also have an anthropic origin or derive from evaporite deposits. The good correlations observed between the EC and bromide ($r^2 = 0.96$), lithium ($r^2 = 0.87$) or strontium ($r^2 = 0.84$) suggests that part of these elements derive from the dissolution of salts, but it also reveals that their groundwater concentrations are at least partly controlled by processes leading to the evapoconcentration of the dissolved species.

4.5.4 Assessment of groundwater salinization processes from mass balance evaluation

Groundwater generally originates from meteoric water, which is poorly mineralized. However, despite flowing in a crystalline environment with relatively short residence times (a few decades in 80% of the borewells investigated, up to a few hundred years), the groundwater is marked by high mineralization levels and chloride concentrations, as well as the predominance of the chloride anion facies. These characteristics are not compatible with the equilibrium time required for the interaction between rock and water to take place to such extent. Indeed, groundwater from igneous or metamorphic rocks normally exhibits low mineralization ($100 - 300 \text{ mg L}^{-1}$), with a predominance of bicarbonate and calcium ions, or even magnesium or sodium cations, whether in temperate climates (Gustafson and Krásný, 1994; Blum et al., 2001) or in semi-arid conditions (Ousmane et al., 1984; Asomaning, 1992; Babaye et al., 2019).

Bicarbonate present in water is generally derived from the hydrolysis of silicate or the dissolution of carbonate minerals, while the presence of calcium, magnesium and potassium is generally attributed to the hydrolysis of plagioclases (source of Na^+ and Ca^{2+}), K-feldspars and/or ferromagnesian minerals such as biotite (source of K^+ and Mg^{2+}), amphiboles, pyroxenes or olivine (sources of Mg^{2+} and Ca^{2+}), among others. The predominance of sodium ions in the crystalline aquifer groundwaters (as observed in our case or in other areas of the world) is generally explained by the presence of alkali feldspars (such as albite or anorthoclase, for example), by reverse cation exchange phenomena (replacement of Ca^{2+} or Mg^{2+} by Na^+) or by calcite and dolomite precipitation phenomena (precipitation of Ca^{2+} and/or Mg^{2+}).

An analysis of the chemical ratios between ions was performed to identify potential sources of groundwater salinization by sorting the samples into ten groups according to facies trends for the sake of clarity: groups 1 to 4 correspond to the least salty waters whose dominant or almost dominant anion is HCO_3^- , while groups 5 to 10 represent the waters whose dominant or almost dominant anion is Cl^- . More details on the group constitution are given in Table 2. These analyses showed that mineral hydrolysis cannot explain the high salinities of the aquifers, but can explain the basic mineralization and the bicarbonate facies of the less salty waters. Indeed, the relationship in meq L^{-1} between Alkalinity + SO_4 and $\text{Ca}^{2+} + \text{Mg}^{2+}$ (Fig. 7 a) underlines that groundwater samples from groups 1 to 4 are close to or below the 1:1 equiline, indicating a deficit in calcium and magnesium. This observation suggests that these ions could come from the hydrolysis of the silicate minerals, and possibly from sulphur-rich minerals (for sulphate), considering the absence of primary carbonates in the crystalline aquifers. The deficit in calcium and magnesium observed for the samples n°144, 164, P17 and 45 is also associated with an excess of sodium in relation to chloride (Fig. 7 b), which indicates an additional source of sodium to that from atmospheric inputs (blue dotted line) or halite dissolution (black dotted line). Analyses suggest that the deficit in calcium and magnesium in relation to the Alkalinity + SO_4 could be

explained by cationic exchange phenomena with clays (Fig. 8 a), or by the albite weathering of the crystalline rocks, which generates bicarbonate ions associated with sodium ions, as described in Equation Eq.6:



The P17 borewell sample (group 2), corresponding to the lowest EC value ($\text{EC} = 886 - 1059 \mu\text{S cm}^{-1}$) is the only perfectly balanced borewell that does not present evidence of contamination by nitrate: the chloride content and a part of the sodium are derived from atmospheric inputs while the others ions (including the other part of sodium) are essentially derived from silicate weathering and cationic exchange. Even if this sample is isotopically marked by evaporation ($\text{d-exc} < -6 \text{ ‰}$), which suggests a possible concentration of the dissolved elements by evaporation, we can assume that the reference values for the crystalline groundwater of the Ceará, when not subjected to salinization or contamination issues, are characterized by a sodium-bicarbonate facies, a total dissolved solids (TDS) content $< 700 \text{ mg L}^{-1}$ and chloride concentration $< 30 \text{ mg L}^{-1}$ (Table 3). Therefore, chloride concentration above this limit may indicate additional salinization processes.

The mineral hydrolysis process can no longer explain the origin of the cations for the salty groundwaters of groups 5 to 10, whose dominant ion is chloride. Indeed, groundwater samples from groups 6 and 8 ($\approx 1700 < \text{EC} < 3500 \mu\text{S cm}^{-1}$) are close to (or slightly above) the 1:1 equiline (Fig. 9 b, d), while samples from groups 5, 7, 9 and 10 ($\approx 1100 < \text{EC} < 14\,300 \mu\text{S cm}^{-1}$) present a strong excess in Ca^{2+} and Mg^{2+} (from 2 to 90 meq L^{-1}) compared to bicarbonate (Fig. 9 a, b), as well as a strong deficit in sodium compared to chloride (Fig. 9 c, d). Results suggest that part of the mineralization originates from silicates hydrolysis, while another part is linked to other processes. Indeed, samples from groups 6 and 8 show a chemical signal that derives from the hydrolysis of silicate minerals but also from the dissolution of salts of halite (and probably of calcite and dolomite, considering the sequence of precipitation of salts). Samples from group 10

also show a signal of halite dissolution. Samples from the groups 5, 7 and 9 of mixed cationic facies (generally $\text{Na}^+ > \text{Mg}^{2+} > \text{Ca}^{2+}$) present a chloride excess in relation to sodium ranging from a few meq L^{-1} to 100 meq L^{-1} , and is particularly significant for solutions above $20 \text{ meq}_{\text{Cl}} \text{ L}^{-1}$ (corresponding to solutions whose $\text{EC} > 3200 \mu\text{S}\cdot\text{cm}^{-1}$). Then, the additional source of Ca^{2+} and Mg^{2+} and the deficit of Na^+ might be explained by reverse cationic exchange phenomena between calcium and magnesium with sodium (adsorption of Na^+ in exchange for bound Ca^{2+} and Mg^{2+} , Fig. 8 b). Alternatively, the sodium deficit may be linked to the dissolution of more evolved salts such as MgCl_2 (or CaCl_2 from fertilizers), which is possible considering the good correlation of these cations with the chloride ($r^2 > 0.7$).

Similar observations were made by Laraque (1991) for the surface water of the study region: water with low mineralization presented a calcium-bicarbonate or sodium-bicarbonate facies, while water with higher mineralization mainly presented a sodium-chloride facies. The salinization of surface water were attributed to the leaching of salt derived from rainfall that were accumulated in the watershed, to the strong evaporation rates, the inadequate sizing of dams and the irregular use of the water contained in the latter (Laraque, 1991).

4.5.5. Evaluating groundwater salinization processes from principal component analyses (PCA)

Two sets of PCA computations were performed to evaluate the relationships between variables and to quantify the contribution of each variable in the constitution of the factorial axes. The first analysis considered all major ions (Fig. 10 a), while the second also took into account the main trace elements (Fig. 10 b). Results show that the variance expressed by the factorial axes F1-F2 is quite significant in both cases and can explain more than 70 % of the initial information. Indeed, more than 55 % (Fig. 10 a) or 75 % (Fig. 10 b) of the variance is controlled by the F1 axis, which is defined by EC, Cl^- , Br^- , Ca^{2+} , Mg^{2+} , Na^+ , K^+ , Sr^{2+} and Li^+ . The grouping of these ele-

ments around the F1 axis materializes a common origin and reflects the mineralization of water attributed to the dissolution of salts. The F2 axis, which explains 13 to 15 % of the variance, is represented on the one hand, by NO_3^- and/or SO_4^{2-} , which represent the impact of human activities and, on the other hand, by HCO_3^- , Si^{4+} , Ba^{2+} and/or SO_4^{2-} , which reflect the mineralization of water due to the hydrolysis of silicate or sulphur-rich minerals. Thus, the PCA outcome supports the hypothesis that the substantial salt concentrations found in the crystalline waters may not be due to the mineral hydrolysis, but may be due to the dissolution of salts. This hypothesis is supported by the observation of saline crusts constituted by evaporite minerals (calcite, dolomite, gypsum, halite and magnesium salts as bischofite) on the banks and sediments of dry reservoirs (Laraque, 1991; Araújo, 2017).

5. Discussion

The first and unprecedented hourly piezometric data acquired in the region evidenced that the seasonal piezometric fluctuation is often continuous and inertial, even if abrupt variations were also detected in some wells (rapid vertical infiltration during the highest rain events). Similarly to other semi-arid regions in the world (Leduc et al., 1998; Babaye et al., 2019; Lachassagne et al., 2021; Goswami & Sekhar, 2022), the recharge of Ceará crystalline aquifers does not directly depend on the amount of annual or monthly rainfall, but on the intensity and distribution of rainfall events, parameters that will both influence the production of surface runoff and surface water accumulation in temporary rivers and dams, and the consequent localized aquifer recharge. Indeed, the isotopic investigation evidenced that groundwater recharge is mainly constituted by localized infiltration of evaporated surface water. This observation, based on 654 recent isotopic analyses leads to a conclusion contrary to the interpretations formulated by Frischkorn et al. (1989), Santiago et al. (2001) and Moura (2013), who concluded from a more limited set of analyses, that the crystalline aquifer recharge is due to direct (diffuse) infiltration without any sign of evaporation of the surface water.

Among the processes that can lead to a salinization of groundwater, marine intrusions and dissolution of marine evaporite rocks are ruled out, considering the distance of the study area from the sea (≈ 180 km) and the absence of primary evaporitic terms in the Precambrian rocks (Almeida et al., 2008). Dating of the groundwater through our multi-tracer approach (^{14}C , ^3H , CFC and SF_6) and the seasonal variations of stable isotopes (^{18}O and ^2H) highlighted that the circulation of groundwater is relatively fast (mean residence time from a few decades to hundreds of years, with a large contribution of post-1950s water) and corroborate the water dating obtained by Santiago et al. (2000). It also showed that the apparent age of the crystalline aquifers waters are function of the annual renewal rate of the aquifer via vertical flows. The hypothesis of a past marine transgression is incompatible with the apparent age of the water, considering that the last marine transgression that possibly reached the study area, and whose witnesses could have been removed by the erosion processes, dates from the Upper Cretaceous (≈ 70 Ma; Arai, 1999). Furthermore, the stable isotopes are incompatible with the hypothesis of mixing with seawater, geothermal flows or fluid inclusions as potential processes of water salinization.

Mineral hydrolysis of the crystalline rocks explains part of the mineralization of the water, but does not account for the significant salinization of the groundwater, contrary to what was suggested by Araújo (2017). Indeed, it was demonstrated in our study that dominant mineral hydrolysis is only associated with low mineralization ($< 700 \text{ mg L}^{-1}$) and bicarbonate facies. Therefore, brackish or saline water with chloride or mixed facies within the crystalline rocks is a consequence of other salinization processes. Chloride is not representative of crystalline rocks, and the presence of brine, fluid inclusions or evaporite rocks does not correspond to the lithological types of the studied region. Consequently, the chloride sources are external to the crystalline aquifer, as evoked by Matsui (1978), Silva (2003) and Britto Costa et al., (2006). It was evidenced in this study that anthropic contamination is not a determining factor in the processes of salinization of water, even if it can contribute to a local degradation of water quality, more spe-

cifically in terms of nitrate content. Therefore, the most likely hypothesis in this context is that the chloride source, hence, the groundwater salinity, is derived from meteoric inputs, whether in the form of wet deposition (during the rainy season) or dry deposition (during the dry season, when most winds occur). Our piezometric monitoring showed that small rainfall events are completely recycled by evapotranspiration and do not contribute to the recharge. Considering the low permeability of soils and the presence of Hortonian-type runoff, most of the chloride deposited on the soil surface may be leached by surface runoff and transferred to surface water reservoirs (rivers, dams, ponds) which are subject to partial or total evaporation. The evaporation of these surface waters can even lead to the local precipitation of evaporite minerals and saline crusts. Indeed, previous studies (Laraque, 1991; Araújo, 2017) evidenced the presence of evaporite minerals (calcite, dolomite, gypsum, halite) on the banks of dried reservoirs, as well as in the clays and sediments of the reservoirs (and probably in the USZ). Saline crusts also contained magnesium salts (probably bischofite $\text{MgCl}_2 \cdot 6\text{H}_2\text{O}$; Araújo, 2017).

The increase in EC observed after the rainy season in most groundwaters, associated with the rise in the piezometric level and the infiltration of partly evaporated surface water, suggests that the seasonal dynamics of water salinity comes from the leaching of salts from the surface. This increase varies from year to year, and suggests that the annual amount of salts leached into the aquifer must be variable and a function of the spatio-temporal distribution of daily rainfall. In terms of salinization processes, these new observations highlight the hypothesis according to which the salinity of recharge waters would be due to the accumulation of salts in localized areas, which will progressively concentrate, either in surface waters (rivers, dams), in the soil or the USZ, due to the high evaporation rates associated with the semi-arid climate, and being leached into the aquifer after more significant rainfall events..

6. Conclusion and perspective

In this multidisciplinary study, piezometric, hydrochemical, isotopic data and multi-tracer dating (^{18}O , ^2H , ^3H , ^{14}C , CFC, SF_6), provided new hydrogeological information, especially about the hydrogeological functioning and the salinization processes of the crystalline aquifers. The high piezometric reactivity of aquifers in response to rainfall marks the seasonal recharge, even during the driest years. The stable isotopes (^{18}O , ^2H) revealed that groundwater is systematically marked by evaporation, confirming that recharge comes from a mixing of evaporated surface waters (localized recharge in lowlands or from surface water bodies) and, to a lesser extent, diffuse recharge of rainwater. Thus, preferential infiltration from localized areas more propitious to infiltration, such as river beds, alluvium, reservoirs or local depressions, is the main pathway of recharge of these aquifers. The determination of groundwater residence times through a multi-tracer approach (^3H , ^{14}C , CFC, SF_6) underlined that the apparent groundwater age is recent and composed of seasonal vertical infiltration flows (direct and indirect) that mix with older waters stored in the aquifer, whose infiltration occurred before the 1960s, and which flow much more slowly.

Although the crystalline aquifers groundwaters are apparently young, they are characterized by high salinities and present essentially mixed-chloride or sodium-chloride facies. Chemical data reveal that groundwater initially exhibits a mixed-bicarbonate or sodium-bicarbonate facies resulting from the hydrolysis of the aquifer crystalline rocks and cation exchange, resulting in EC values that should not exceed $1000 \mu\text{S cm}^{-1}$. However, the partial or total evapo(transpi)ration of small rainfall events and surface waters favours the concentration of the atmospheric salts deposited onto the soil, and in the USZ, the sediments of the ponds and/or the surface waters, causing eventually their precipitation in the form of evaporitic salts, such as calcite, dolomite, gypsum, halite or even more evolved salts such as MgCl_2 (indicating the strong evaporation rates that can locally affect the waters before their infiltration). The dissolution and leaching of these evapoconcentrated salts into the aquifers during more intense rainfall events

shift the groundwater facies from the bicarbonate pole to the chloride pole. Therefore, the geochemical interpretations showed that the origin of the groundwater salinization is not linked to the hydrolysis of crystalline rock minerals, but to the lixiviation of evapoconcentrated salts into the aquifer. Reverse cationic exchange processes can affect the groundwater composition, but not the degree of salinization. Moreover, anthropogenic pollution can contribute locally to the degradation of the water quality (more specifically in terms of nitrate), but has not been identified as a determining factor in the salinization processes.

In light of these conclusions, the perspectives of this study are to test with a quantitative model if the hypothesis of atmospheric inputs concentrated locally by evapotranspiration allow to reach the observed salinities, and also to evaluate the possible influences of surface water evaporation or other phenomena such as the transpiration of groundwater (from the saturated zone) by the vegetation (Herczeg et al., 2001; Favreau, 2018) on groundwater salinity. Such a quantitative modelling of the salinization processes was performed in the frame of the continuation of this research (Kreis et al., under revision).

Acknowledgements

This work is part of the multidisciplinary French-Brazilian cooperation between IRD and FUNCEME, and was carried out in the frame of a PhD research. The authors would like to thank the FUNCEME for all the financial and technical support of the field work, as well as the FUN-CAP for the scholarship provided. The authors also want to give credit to the LAMA, Condate Eau-OSUR, EMMAH and AETE-ISO laboratories for the analytical support.

Disclosure statement

The authors declare that they have no conflict of interest.

References

- Ahmed AA, Shabana AR, & Saleh AA (2019). Using hydrochemical and isotopic data to determine sources of recharge and groundwater evolution in arid region from Eastern Desert, Egypt. *J. of Afr. Earth Sci.*, 151, 36-46. <https://doi.org/10.1016/j.jafrearsci.2018.11.024>
- Alazard M, Boisson A, Maréchal JC, Perrin J, Dewandel B, Schwarz T, ... & Ahmed S (2016). Investigation of recharge dynamics and flow paths in a fractured crystalline aquifer in semi-arid India using borehole logs: implications for managed aquifer recharge. *Hydrogeol. J.*, 24(1), 35-57. <https://doi.org/10.1007/s10040-015-1323-5>
- Almeida AR, Parente CV, Arthaud MH (2008). Geologia da folha Quixeramobim SB.24-V-D-III. Programa geologia do Brasil, levantamentos geológicos básicos. Escala 1:100.000, nota explicativa integrada com Boa Viagem e Itatira. CPRM/UFC. 196p.
- American Public Health Association - APHA (2012) Standard methods for the examination of water and wastewater. 22th edition. Wahington, DC. 2012. 1100p.
- Arai M (1999). A transgressão marinha mesocretácea: sua implicação no paradigma da reconstituição paleogeográfica do Cretáceo no Brasil. Simpósio sobre o Cretáceo do Brasil, 5(1999), 577-582.
- Araújo A (2017). Mecanismos dominantes na salinização de água em rochas anisotrópicas com base em razões iônicas e número fuzzy, em área do sertão central no Ceará. Thesis (PhD). Programa de Pós-Graduação em Geologia da Universidade Federal do Ceará, 188p.
- Asomaning G (1992). Estudo comparativo sobre as condições hidrogeológicas das rochas pré-cambrianas nos estados da Paraíba e São Paulo, Brasil e Gana, África ocidental. Thesis (PhD), Universidade de São Paulo – Instituto de Geociências (Brasil). 201p.
- Babaye MSA, Orban P, Ousmane B, Favreau G, Brouyère S & Dassargues A (2019). Characterization of recharge mechanisms in a Precambrian basement aquifer in semi-arid southwest Niger. *Hydrogeol. J.*, 27(2), 475-491. <https://doi.org/10.1007/s10040-018-1799-x>
- Banyikwa AT (2023). Evaluation of hydrogeochemical characteristics, spatial distribution of major ions, and water quality for drinking and irrigation in six districts of the Dodoma region in Tanzania. *Groundw. Sustain. Dev.*, 100897. <https://doi.org/10.1016/j.gsd.2022.100897>
- Basavarajappa HT & Manjunatha MC (2015). Groundwater quality analysis in Precambrian rocks of Chitradurga district, Karnataka, India using Geo-informatics technique. *Aquat. Procedia*, 4, 1354-1365. <https://doi.org/10.1016/j.aqpro.2015.02.176>

- Blavoux B, Lachassagne P, Henriot A, Ladouche B, Marc V, Beley JJ, Nicoud G & Olive P (2013). A fifty-year chronicle of tritium data for characterising the functioning of the Evian and Thonon (France) glacial aquifers. *J. of hydrol.*, 494, 116-133. <https://doi.org/10.1016/j.jhydrol.2013.04.029>
- Blum A, Barbier J, Chery L, Petelet-Giraud E (2001). Contribution à la caractérisation des états de référence géochimique des eaux souterraines. Outils et méthodologie. Rapport BRGM/RP-51093-FR, 286p.
- Britto Costa AM, de Melo JG & da Silva FM (2006). Aspectos da salinização das águas do aquífero cristalino no estado do Rio Grande do Norte, Nordeste do Brasil. *Águas Subterrâneas*, 20(1).
- Burte JDP (2008). Os pequenos aquíferos aluviais nas áreas cristalinas semiáridas: funcionamento e estratégias de gestão. Estudo de caso no Nordeste Brasileiro. Thesis (PhD), Universidade Federal do Ceará (Brasil) - Université Montpellier 2 (França). 194p.
- Cartwright I, Weaver TR & Fifield LK (2006). Cl/Br ratios and environmental isotopes as indicators of recharge variability and groundwater flow: an example from the southeast Murray Basin, Australia. *Chem. Geol.*, 231(1-2), 38-56.
- Crosbie RS, Binning P & Kalma JD (2005). A time series approach to inferring groundwater recharge using the water table fluctuation method. *Water Resour. Res.*, 41(1). <https://doi.org/10.1029/2004WR003077>
- Da Silva AJP, Lopes RCL, Vasconcelos AM, Bahia RBC (2003). Capítulo II – Bacias sedimentares paleozoicas e meso-cenozoicas interiores in: *Geologia, Tectônica e Recursos Minerais do Brasil*. CPRM: Brasília. 55-85.
- Da Silva FJA, de Araújo AL & de Souza RO (2007). Águas subterrâneas no Ceará—poços instalados e salinidade. *Revista Tecnologia*, 28(2).
- Da Silva MJ, Galvêncio JD, Costa VSO (2017). Abordagem interdisciplinar sobre a influência da zone de convergência intertropical – ZCIT no Nordeste Brasileiro. *Revista Mov. Sociais e Dinâmicas Espaciais, Recife*, V.6, N.1, 107-117.
- Da Silva Nobre ME, Gomes DF, Vasconcelos SMS, de Lima Neto IO, Ferreira SK, & de Ponti Souza D (2019). Estudo hidroquímico-ambiental do aquífero aluvionar do baixo Jaguaribe, Itaíba—Ceará. *Revista do Instituto Geológico*, 39(3), 77-92.
- Dewandel B, Perrin J, Ahmed S, Aulong S, Hrkal Z, Lachassagne P, Samad M & Massuel S (2010). Development of a tool for managing groundwater resources in semi-arid hard rock regions: application to a rural watershed in South India. *Hydrol. Process.*, 24(19), 2784-2797. <https://doi.org/10.1002/hyp.7696>

- Drever JI, 1997. *The Geochemistry of Natural Waters: Surface and Groundwater Environments*. Prentice-Hall, New Jersey, USA. 436 pp.
- Favreau G (2018). *Momentum et paradoxa: impacts du climat et de l'occupation des sols sur les aquifères au Sahel*. Montpellier : IRD, 116 p. multigr. Mém. HDR. Habilitation à Diriger des Recherches, Univ. de Montpellier. 2018/05/07.
- Feitosa FAC, Manoel Filho J, Feitosa EC & Demetrio JGA (2008). *Hidrogeologia: conceitos e aplicações*. 3. ed. Revisada e ampliada. Rio de Janeiro: CPRM: LABHID, 2008. 812p.
- Freitas Filho MR & Carvalho MSBS (2021). *Mapeamento das barragens dos pequenos reservatórios d'água situados no Estado do Ceará*. Relatório Técnico. Fortaleza: Funceme: 10p.
- Frischkorn H, Santiago MF, & Serejo AN (1989). Isotope study of wells in crystalline rock of the semi-arid northeast of Brazil. *Regional Seminar for Latin America on the Use of Isotope Techniques in Hydrology*, 73-89.
- Frischkorn H & Santiago MF (2000). Mechanisms of Salinization in the North of Brazil. In *German-Brazilian Workshop on Neotropical Ecosystems—Achievements and Prospects of Cooperative Research*, Hamburg, 497-503.
- Fundação Cearense de Meteorologia e Recursos Hídricos - Funceme (2007). *Mapeamento e Avaliação do Potencial Hídrico Subterrâneo dos Aluviões em Zonas SemiÁridas Utilizando Técnicas de Sensoriamento Remoto e SIG*. Fortaleza: Governo do Estado do Ceará. Available from: <http://www.funceme.br/wp-content/uploads/2019/02/Aluviao.pdf>
- Goswami S & Sekhar M (2022). Investigation and evidence of high episodic groundwater recharge events in tropical hard-rock aquifers of southern India. *Front. Water*, 4. <https://doi.org/10.3389/frwa.2022.960669>
- Guihéneuf N, Boisson A, Bour O, et al. (2014). Groundwater flows in weathered crystalline rocks: Impact of piezométric variations and depth-dependent fracture connectivity. *J. of Hydrol.* 2014;511:320-334. <https://doi.org/10.1016/j.jhydrol.2014.01.061>
- Gustafson G & Krásný J. (1994). Crystalline rock aquifers: their occurrence, use and importance. *Appl. Hydrogeol.*, 2(2), 64-75. <https://doi.org/10.1007/s100400050051>
- Healy RW & Cook PG (2002). Using groundwater levels to estimate recharge. *Hydrogeol. J.*, 10(1), 91-109. <https://doi.org/10.1007/s10040-001-0178-0>
- Herczeg AL, Dogramaci SS & Leaney FWJ (2001). Origin of dissolved salts in a large, semi-arid groundwater system: Murray Basin, Australia. *Marine and Freshwater Research*, 52(1), 41-52. <https://doi.org/10.1071/MF00040>
- INESP (2009). *Caderno regional da sub-bacia do Banabuiú*. Volume 2. Fortaleza: INESP; 116p.

- Kloppmann W, Bourhane A & Asfirane F (2011). Méthodologie de diagnostic de l'origine de la salinité des masses d'eau. Emploi des outils géochimiques, isotopiques et géophysiques. BRGM/RP-60026-FR.
- Kreis M, Taupin JD, Patris N & Martins ESPR (2020). Isotopic characterisation and dating of groundwater recharge mechanisms in crystalline fractured aquifers: example of the semi-arid Banabuiú watershed (Brazil). *Isot. in Environ. and Health Studies*, 56(5-6), 418-430. <https://doi.org/10.1080/10256016.2020.1797275>
- Kreis M (2021). Origine et dynamique de salinité des aquifères fracturés cristallins de la région semi-aride du Ceará, Brésil. Thesis (PhD), Université de Montpellier (France), Universidade federal do Ceará (Brasil). 440p.
- Kreis M, Taupin JD, Lachassagne P, Patris N & Martins ESPR (under revision). Transpiration of crystalline unconfined aquifers in a semi-arid area is the cause of groundwater salinization. *Hydrogeol. J.*
- Lachassagne P, Wyns R & Dewandel B (2011). The fracture permeability of hard rock aquifers is due neither to tectonics, nor to unloading, but to weathering processes. *Terra Nova*, 23(3), 145-161. <https://doi.org/10.1111/j.1365-3121.2011.00998.x>
- Lachassagne P, Dewandel B & Wyns R (2021). Hydrogeology of weathered crystalline/hard-rock aquifers - guidelines for the operational survey and management of their groundwater resources. *Hydrogeol. J.*, 1-34. <https://doi.org/10.1007/s10040-021-02339-7>
- Laraque A (1991). Comportements hydrochimiques des "açudes" du Nordeste brésilien semi-aride: évolutions et prévisions pour un usage en irrigation. Thesis (PhD), Université de Montpellier 2 (France). 446p.
- Leduc C, Salifou O, Leblanc M (1998). Evolution des ressources en eau dans le département de Diffa (bassin du lac Tchad, Sud-Est nigérien). Servat, E., Hughes, D., Fritsch, J. M., and Hulme, M.. Conference Proceeding Water resources variability in Africa during the 20th century. IAHS Publ. 252, Wallingford, 281-288.
- Manoel Filho J (1996). Modelo de dimensão fractal para avaliação de parâmetros hidráulicos em meio fissural. Thesis (PhD), Universidade de São Paulo.
- Marçais J, Gauvain A, Labasque T, Abbott BW, Pinay G, Aquilina L, Chabaux F, Viville A & de Dreuzy JR (2018). Dating groundwater with dissolved silica and CFC concentrations in crystalline aquifers. *Science of the Total Environment*, 636, 260-272. <https://doi.org/10.1016/j.scitotenv.2018.04.196>

- Maréchal JC, Dewandel B, Ahmed S, Galeazzi L, & Zaidi FK (2006). Combined estimation of specific yield and natural recharge in a semi-arid groundwater basin with irrigated agriculture. *J. of Hydrol.*, 329(1-2), 281-293. <https://doi.org/10.1016/j.jhydrol.2006.02.022>
- Maréchal JC, Lachassagne P, Ladouche B, Dewandel B, Lanini S, Le Strat P & Petelet-Giraud E (2014). Structure and hydrogeochemical functioning of a sparkling natural mineral water system determined using a multidisciplinary approach: a case study from southern France. *Hydrogeol. J.*, 22(1), 47-68. <https://doi.org/10.1007/s10040-013-1073-1>
- Martins ESPR & Vasconcelos Júnior FDC (2017). O clima da Região Nordeste entre 2009 e 2017: Monitoramento e previsão. *Parcerias Estratégicas*, 22(44), 63-79.
- Matsui E (1978). Origem e dinâmica de salinização da água do nordeste brasileiro – Bacia do rio Pajeú/PE. Thesis (PhD), Universidade de Sao Paulo. 72p.
- Ministério de Minas e Energia – MME (1998). Programa de recenseamento de fontes de abastecimento por água subterrânea no Estado do Ceará. Diagnóstico do município de Quixeramobim. CPRM: Fortaleza. 15p.
- Ministério do Meio Ambiente – MMA (2007). Atlas das áreas susceptíveis à desertificação do Brasil. Santana, M. O. (organizador). Brasília: MMA/SRH/UFPB. 134p.
- Mizan SA, Dewandel B, Selles A, Ahmed S & Caballero Y (2019). A simple groundwater balance tool to evaluate the three-dimensional specific yield and the two-dimensional recharge: application to a deeply weathered crystalline aquifer in southern India. *Hydrogeol. J.*, 27:3063–3080. <https://doi.org/10.1007/s10040-019-02026-8>
- Molle F & Cadier E (1992). Manual do pequeno açude. Recife : SUDENE ; ORSTOM ; TAPI, 1992, 521 p.
- Moura IBMD (2013). Estudos das águas da bacia hidrográfica do Rio Banabuiú no trecho entre Quixeramobim e Banabuiú, Ceará, Brasil. Thesis (PhD), Universidade Federal do Ceará. 244p.
- Nascimento FJDSC (2016). Zoneamento da magnitude e da variabilidade temporal dos escoamentos como indicador do potencial de regularização de vazão através de açudes. Thesis (Master degree), Instituto Federal do Ceará, Tecnologia em Gestão Ambiental, Campus Fortaleza.
- N'guettia G K, Mangoua JMO, Aboua NK, Douagui AG & Gone LD (2019). Caractérisation hydrogéochimique des eaux souterraines du bassin versant de la Baya, Est Côte d'Ivoire. *Int. J. Biol. Chem. Sci*, 13(1), 574-585. <https://dx.doi.org/10.4314/ijbcs.v13i1.44>
- Ousmane B, Fontes JC, Aranyosy JF & Joseph A (1984). Hydrogéologie isotopique et hydrochimie des aquifères discontinus de la bande sahélienne et de l'Air (Niger). *Isotope Hy-*

- drology 1983, International Symposium on isotope hydrology in water resources development, AIEA Proc. ser. 650, 367-395.
- Peulvast JP, Sales VC, Bétard F & Gunnell Y (2008). Low post-Cenomanian denudation depths across the Brazilian Northeast: implications for long-term landscape evolution at a transform continental margin. *Glob. and Planet. Change*, 62(1-2), 39-60. <https://doi.org/10.1016/j.gloplacha.2007.11.005>
- Pontes Filho JD, Souza Filho FDA, Martins ESPR & Studart TMDC (2020). Copula-Based Multivariate Frequency Analysis of the 2012–2018 Drought in Northeast Brazil. *Water*, 12(3), 834. <https://doi.org/10.3390/w12030834>
- Pradeep K, Nepolian M, Anandhan P, Kaviyarasan R, Prasanna MV, & Chidambaram S (2016). A study on variation in dissolved silica concentration in groundwater of hard rock aquifers in Southeast coast of India. In *IOP Conference Series: Materials Science and Engineering*, Vol. 121, No. 1, 012008. IOP Publishing. <https://doi.org/10.1088/1757-899X/121/1/012008>
- Rabemanana V, Violette S, De Marsily G, Robain H, Deffontaines B, Andrieux P, ... & Parriaux A (2005). Origin of the high variability of water mineral content in the bedrock aquifers of Southern Madagascar. *J. Hydrol.*, 310(1-4), 143-156. <https://doi.org/10.1016/j.jhydrol.2004.11.025>
- Ribeiro Neto GG, Melsen LA, Martins ES, Walker DW & Van Oel PR (2022). Drought Cycle Analysis to evaluate the influence of a dense network of small reservoirs on drought evolution. *Water Resour. Res.*, 58(1), e2021WR030799. <https://doi.org/10.1029/2021WR030799>
- Salati E, LEAO JM & Campos MM (1979a). Isótopos ambientais aplicados a um estudo hidrogeológico do Nordeste brasileiro. Recife: SUDENE/DRN.
- Salati E, Dall'Olio A, Matsui E & Gat JR (1979b). Recycling of water in the Amazon basin: an isotopic study. *Water resour. res.*, 15(5), 1250-1258.
- Santiago MMF, Frischkorn H & Mendes Filho J (2000). Mecanismos de salinização em águas do Ceará, Rio Grande do Norte e Piauí. *Águas Subterrâneas*. Joint World Congress on Groundwater. Anais do XI Congresso Brasileiro de Águas Subterrâneas. <https://aguassubterraneas.abas.org/asubterraneas/article/view/23481>
- Santiago MMF, Frischkorn H, Neto PS & Mendes Filho J (2001). The recharge mechanisms in an alluvial aquifer zone in northeast Brazil. *Ground water*, 39(1), 18-23.

- Scanlon BR, Keese KE, Flint AL, Flint LE, Gaye CB, Edmunds WM & Simmers I (2006). Global synthesis of groundwater recharge in semiarid and arid regions. *Hydrol. Process.*, 20(15), 3335-3370. <https://doi.org/10.1002/hyp.6335>
- Schwiede M, Duijnsveld WHM & Böttcher J (2005). Investigation of processes leading to nitrate enrichment in soils in the Kalahari Region, Botswana. *Phys. and Chem. of the Earth, Parts A/B/C*, 30(11-16), 712-716. <https://doi.org/10.1016/j.pce.2005.08.012>
- Shand P, Edmunds WM, Lawrence AR, Smedley P & Burke S (2007). The natural (baseline) quality of groundwater in England and Wales. Environment Agency. Research Report RR/07/06 and Technical Report NC/99/74/24
- Silva SGD (2003). Aquíferos fissurais em clima semiárido (caso do estado do RN, NE do Brasil): uma análise dos processos de salinização em escala regional e local. Thesis (PhD), Universidade Estadual Paulista, Brasil. 182p.
- Sreedevi PD, Sreekanth PD & Reddy DV (2021). Influence of hydrological and hydrogeological factors on inland groundwater salinity in a hard rock aquifer, south India. *J. Earth Syst. Sci.*, 130(4), 1-15. <https://doi.org/10.1007/s12040-021-01715-x>
- Stolf R (1977). Balanço de água e cloro no açude Quebra-Unhas (PE) utilizando as variações naturais de oxigênio-18, deutério e cloro. Thesis (PhD), Escola Superior de Agricultura Luiz de Queiroz, Universidade de São Paulo, Piracicaba.
- Taupin JD, Gallaire R & Arnaud Y (1997). Analyses isotopiques et chimiques des précipitations sahéliennes de la région de Niamey au Niger: implications climatologiques. *Hydrochem., AISH*, 244, p. 151-162.
- Wyns R, Baltassat JM, Lachassagne P, Legtchenko A, Vairon J & Mathieu F (2004). Application of Proton Magnetic Resonance Soundings to groundwater reserve mapping in weathered basement rocks (Brittany, France). *Bull. Soc. géol. Fr.*, 175 (1), 21-34. <https://doi.org/10.2113/175.1.21>
- Zakaria MG, Taupin JD, Ranaivoarisoa A & Robison LR (2015). Caractérisation géochimique et bactériologique des nappes d'une région à climat tropical sec au centre Sud de Madagascar. *Hydrological Sciences Journal*, 60(4), 746-759. <https://doi.org/10.1080/02626667.2014.932052>

Table 1. Major ion concentrations.

Ion	Median value	Min.	Max.	Standard deviation	Number of samples
Ca ²⁺ (mg L ⁻¹)	154	41	896	183	65
Mg ²⁺ (mg L ⁻¹)	117	19	758	124	65
Na ⁺ (mg L ⁻¹)	275	98	1800	318	65
K ⁺ (mg L ⁻¹)	15	2	49	12	65
Cl ⁻ (mg L ⁻¹)	702	29	5126	1024	65
HCO ₃ ⁻ (mg L ⁻¹)	468	54	941	191	65
SO ₄ ²⁻ (mg L ⁻¹)	45	4	317	57	63
NO ₃ ⁻ (mg L ⁻¹)	71	2	690	113	64
NO ₂ ⁻ (mg L ⁻¹)	0.17	0.03	0.67	0.15	26

Table 2. Groundwater groups identified according to facies trends.

Group	Anion facies	Cation facies	EC range ($\mu\text{S cm}^{-1}$)
1	$\text{HCO}_3^- \rightarrow$ when $[\text{HCO}_3^-] > 50\%$ of anions	Mixed (mainly $\text{Na}^+ \geq \text{Mg}^{2+} \geq \text{Ca}^{2+}$)	1200-1600
2		$\text{Na}^+ \rightarrow$ when $[\text{Na}^+] > 50\%$ of cations	1000-1400
3	$\text{HCO}_3^- - \text{SO}_4^{2-} \rightarrow$ when $[\text{HCO}_3^-] > 40\%$ of anions and presence of sulfate	Mixed ($\text{Na}^+ \geq \text{Ca}^{2+} \geq \text{Mg}^{2+}$)	1000
4	Mixed ($\text{HCO}_3^- > \text{Cl}^-$) \rightarrow when $[\text{HCO}_3^-]$ and $[\text{Cl}^-] > 40\%$ of anions	Mixed (mainly $\text{Na}^+ \geq \text{Mg}^{2+} > \text{Ca}^{2+}$)	1200-2200
5	Mixed ($\text{Cl}^- > \text{HCO}_3^-$) \rightarrow when $[\text{Cl}^-]$ and $[\text{HCO}_3^-] > 40\%$ of anions	Mixed (mainly $\text{Na}^+ > \text{Mg}^{2+} > \text{Ca}^{2+}$)	1800-2300
6	Mixed ($\text{Cl}^- \geq \text{HCO}_3^- > \text{NO}_3^-$) \rightarrow when $[\text{Cl}^-] > 40\%$ of anions and presence of nitrate	Mixed (mainly $\text{Mg}^{2+} \geq \text{Ca}^{2+} \geq \text{Na}^+$)	1700-3200
7	$\text{Cl}^- \rightarrow$ when $[\text{Cl}^-] > 50\%$ of anions	Mixed (mainly $\text{Na}^+ \geq \text{Mg}^{2+} \geq \text{Ca}^{2+}$)	1900-3800
8		$\text{Na} \rightarrow$ when $[\text{Na}^+] > 50\%$ of cations	2900-3500
9	Ultra $\text{Cl}^- \rightarrow$ when $[\text{Cl}^-] > 60\%$ of anions	Mixed (mainly $\text{Na}^+ \geq \text{Mg}^{2+} > \text{Ca}^{2+}$)	2500-14300
10		$\text{Na} \rightarrow$ when $[\text{Na}^+] > 50\%$ of cations	1100-10700

Table 3. Reference values for the groundwater of the crystalline rocks in Ceará that are not subject to pollution or salinization processes.

EC ($\mu\text{S cm}^{-1}$)	Ca²⁺ (mg L^{-1})	Mg²⁺ (mg L^{-1})	Na⁺ (mg L^{-1})	K⁺ (mg L^{-1})	Cl⁻ (mg L^{-1})	HCO₃⁻ (mg L^{-1})	SO₄²⁻ (mg L^{-1})	NO₃⁻ (mg L^{-1})
1059	41	32	135	5	29	573	19	0

ACCEPTED MANUSCRIPT

Figure captions

Figure 1. Localization of the study area and the monitored boreholes.

Figure 2. Location of the sampled points for the isotope and dating analyses. Only borewells that were sampled for groundwater dating have a colored background.

Figure 3. Monitoring of the groundwater levels of the crystalline aquifers between 2011 and 2019.

Figure 4. Hourly piezometric monitoring (Nov. 2016 to Dec. 2019) of the PIR-P14 and IBI-P24 boreholes with associated daily and annual rainfall.

Figure 5. Water isotopic compositions of rainwater, groundwater and surface water.

Figure 6. Piper diagram of the groundwater sampled before (December 2017, 27 samples) and after (June 2018, 38 samples) the rainy season.

Figure 7. (Alkalinity + SO_4^{2-}) vs (Ca^{2+} + Mg^{2+}) (A) and Cl^- vs Na^+ (B) biplots for the bicarbonate type groundwater.

Figure 8. (Ca^{2+} + Mg^{2+} - HCO_3^- - SO_4^{2-}) vs (Na^+ + K^+ - Cl^-) biplot for the bicarbonate type groundwater (A) and the chloride type groundwater (B).

Figure 9. (Alkalinity + SO_4^{2-}) vs (Ca^{2+} + Mg^{2+}) biplot (A, B) and Cl^- vs Na^+ biplot (C, D) for the chloride type groundwater.

Figure 10. Principal Component Analysis (PCA) of variables. Dimension 1 and 2 (Dim 1 and Dim 2) is the space where variables are expressed (>70 % of variance). Variables analysed: EC, Ca^{2+} , Mg^{2+} , Na^+ , K^+ , Cl^- , HCO_3^- , SO_4^{2-} and NO_3^- (A), EC, Ca^{2+} , Mg^{2+} , Na^+ , K^+ , Cl^- , Br^- , Si^{4+} , Ba^{2+} , Sr^{2+} and Li^+ (B).

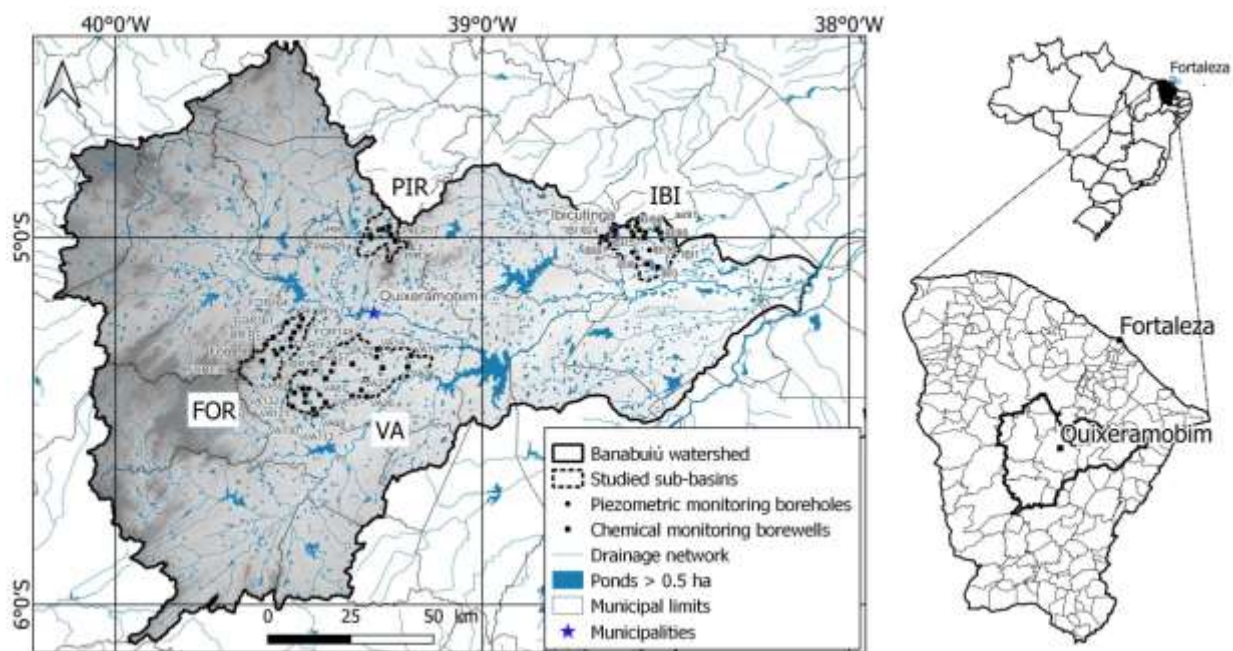


Fig.1

ACCEPTED MANUSCRIPT

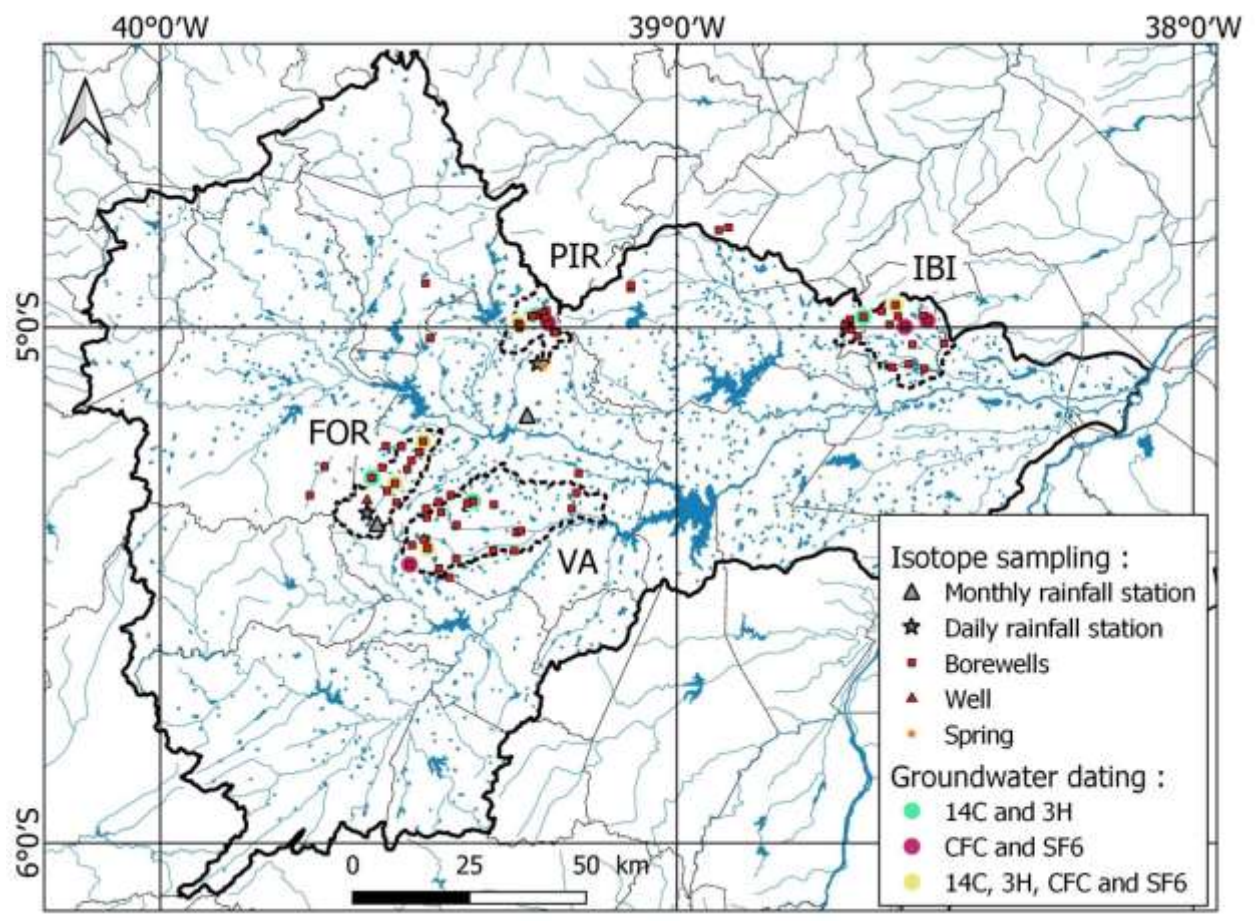


Fig.2

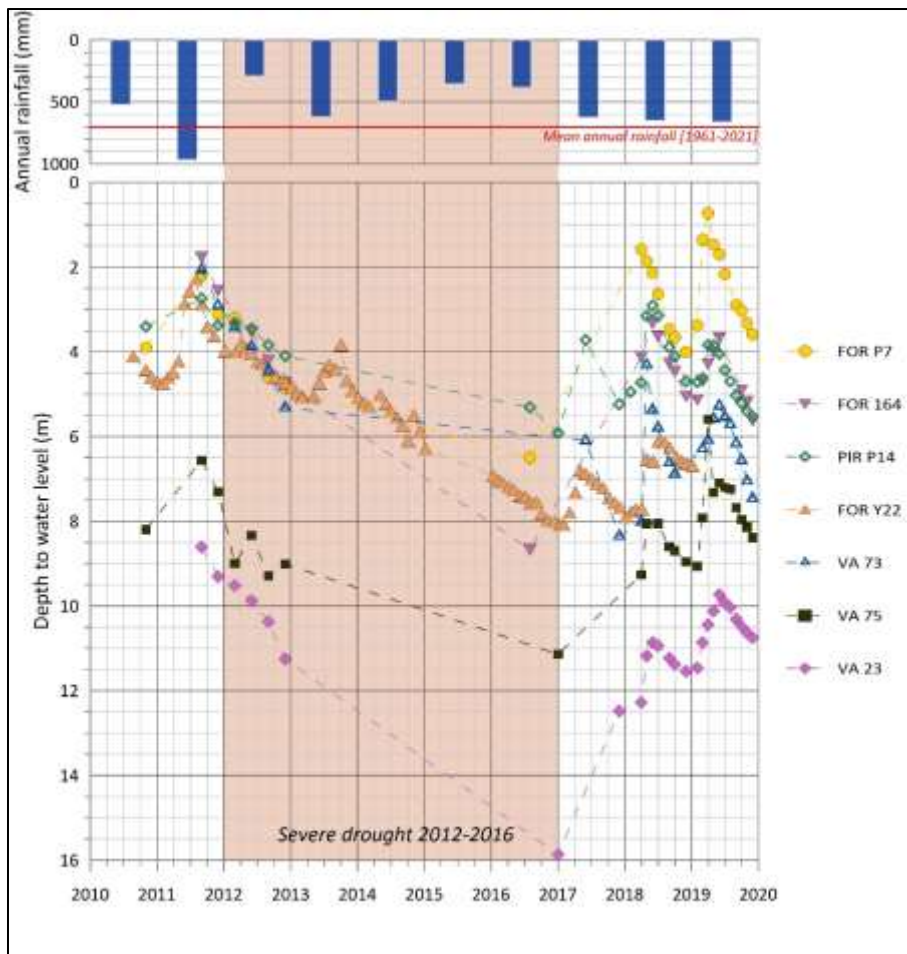


Figure 3

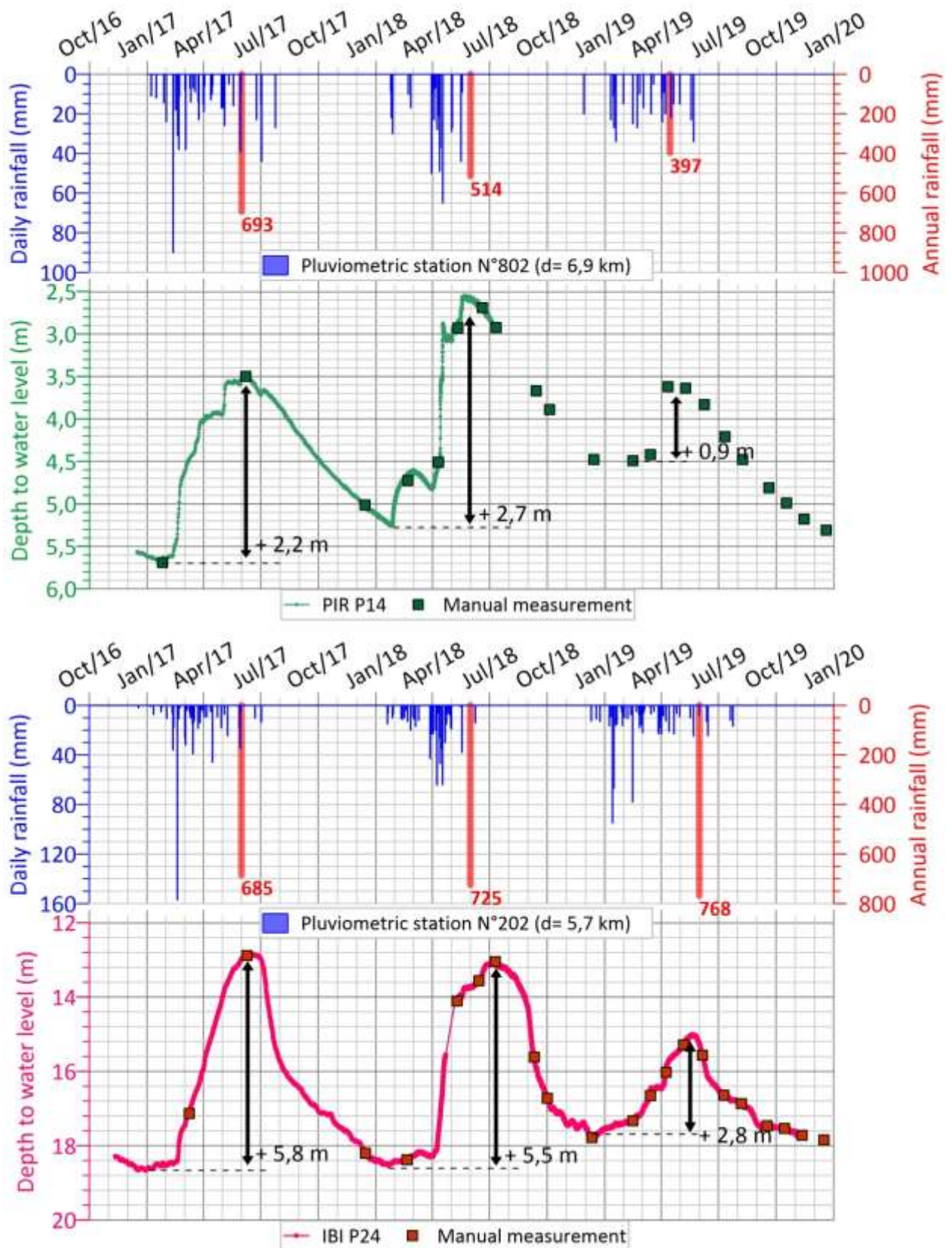


Fig.4

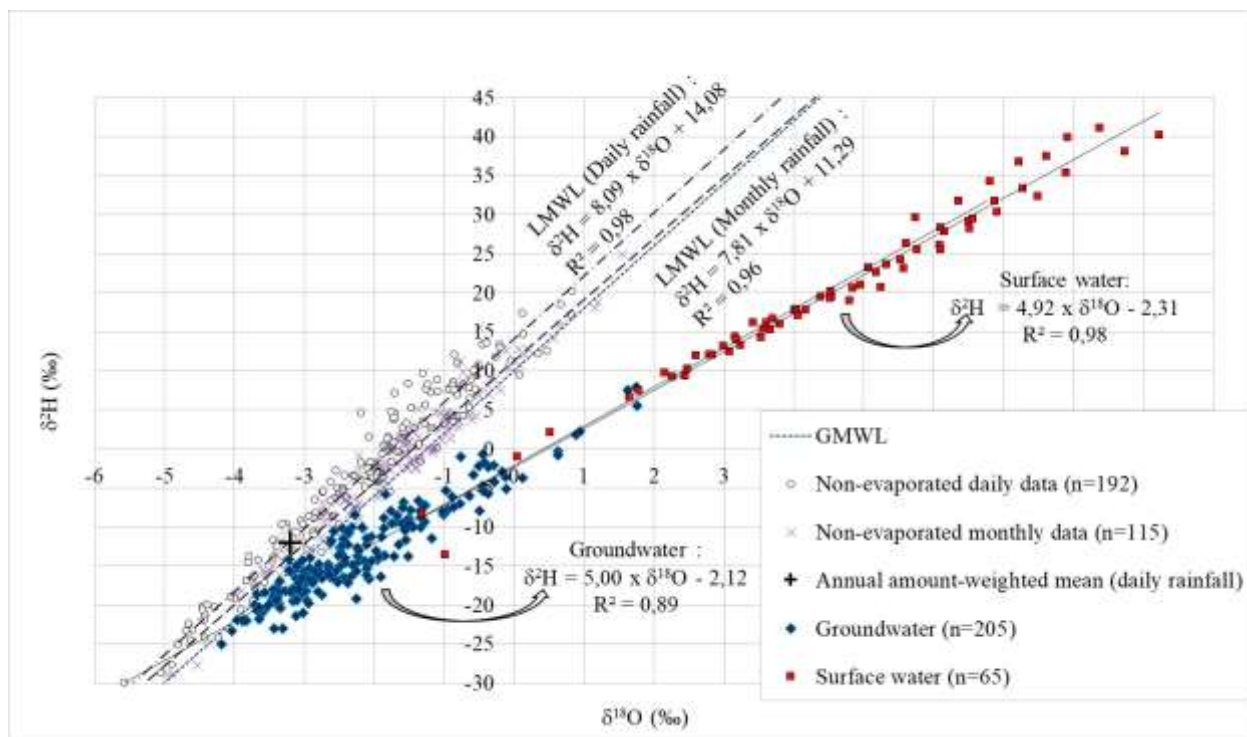


Fig.5

ACCEPTED MANUSCRIPT

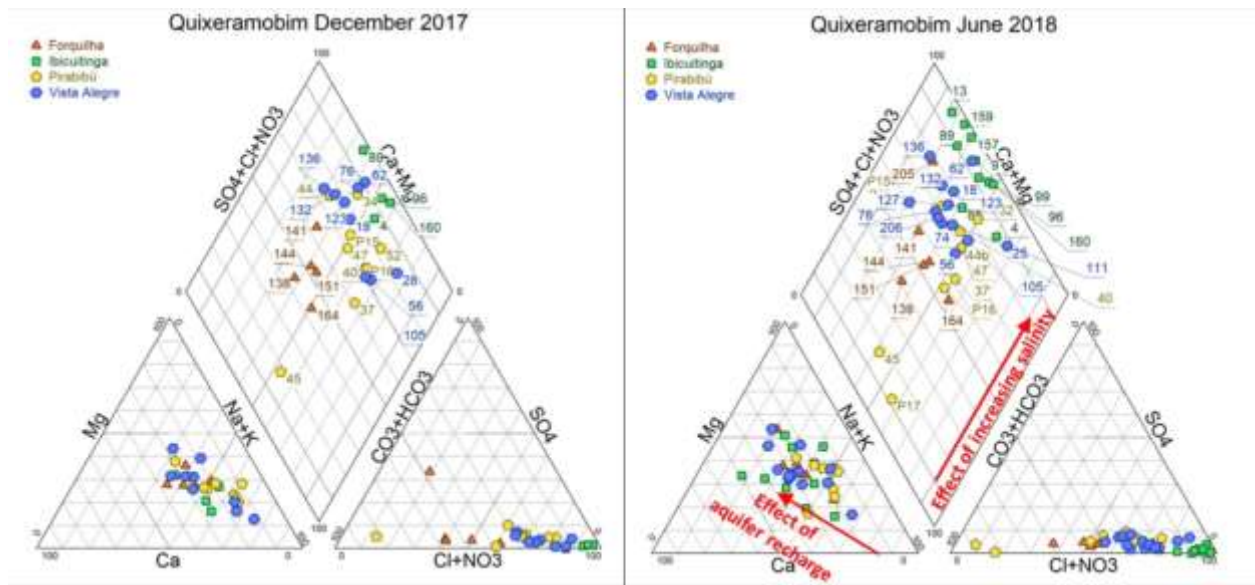


Fig.6

ACCEPTED MANUSCRIPT

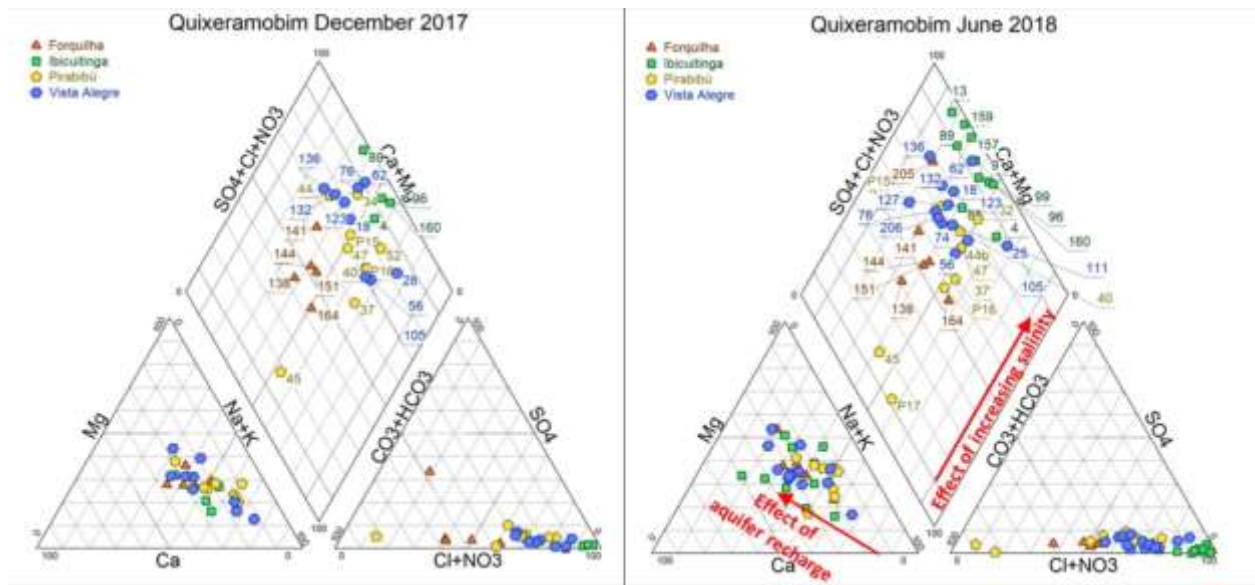


Fig.7

ACCEPTED MANUSCRIPT

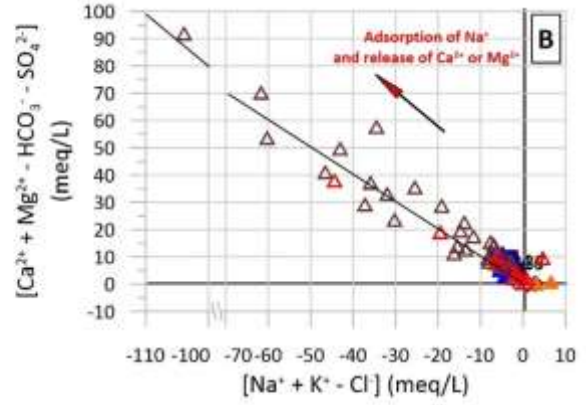
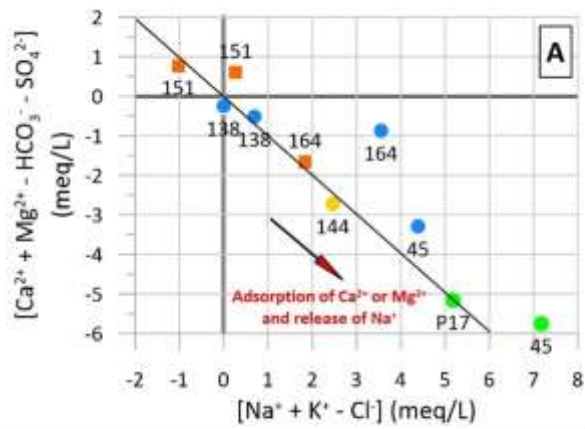


Fig.8

ACCEPTED MANUSCRIPT

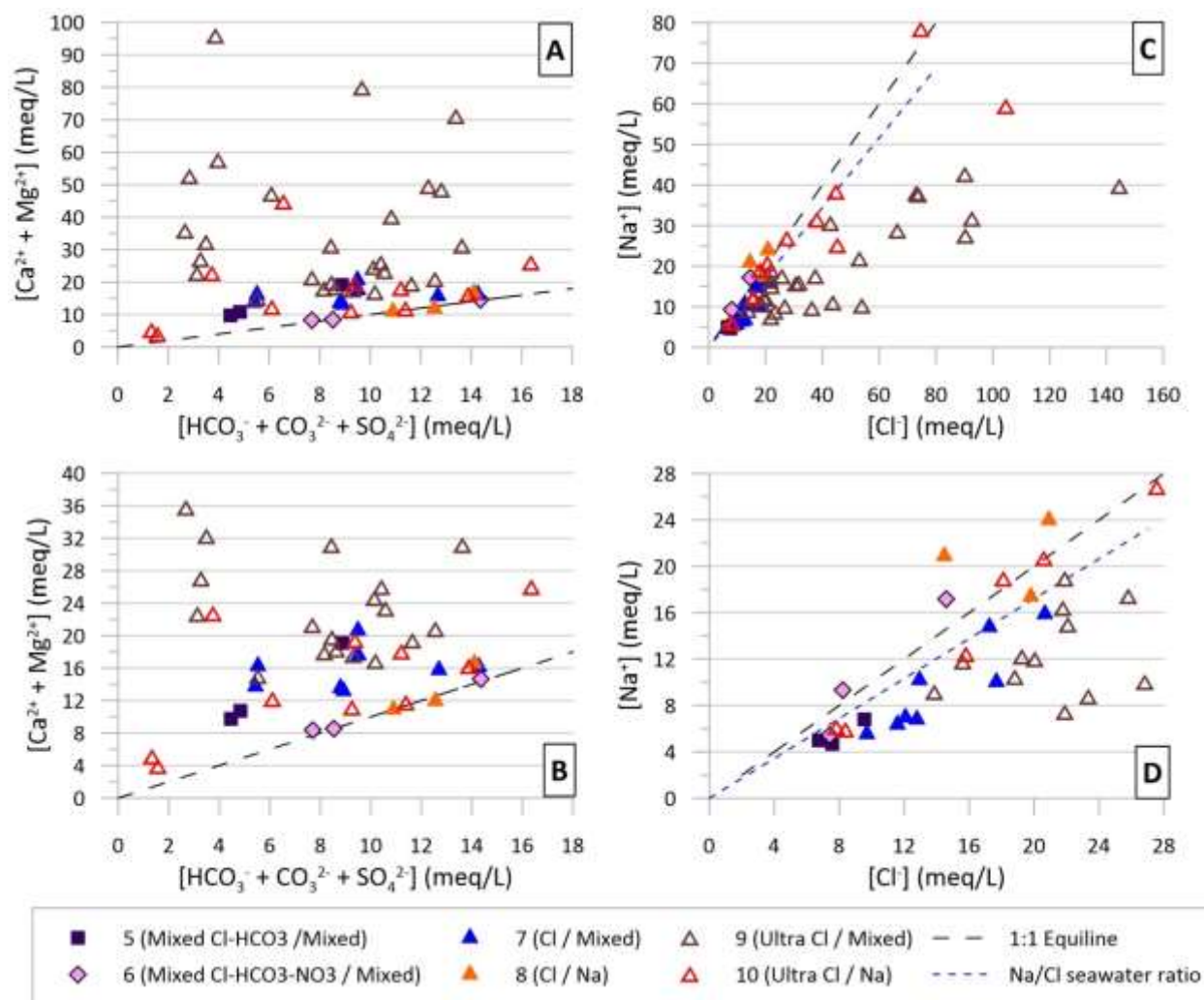


Fig.9

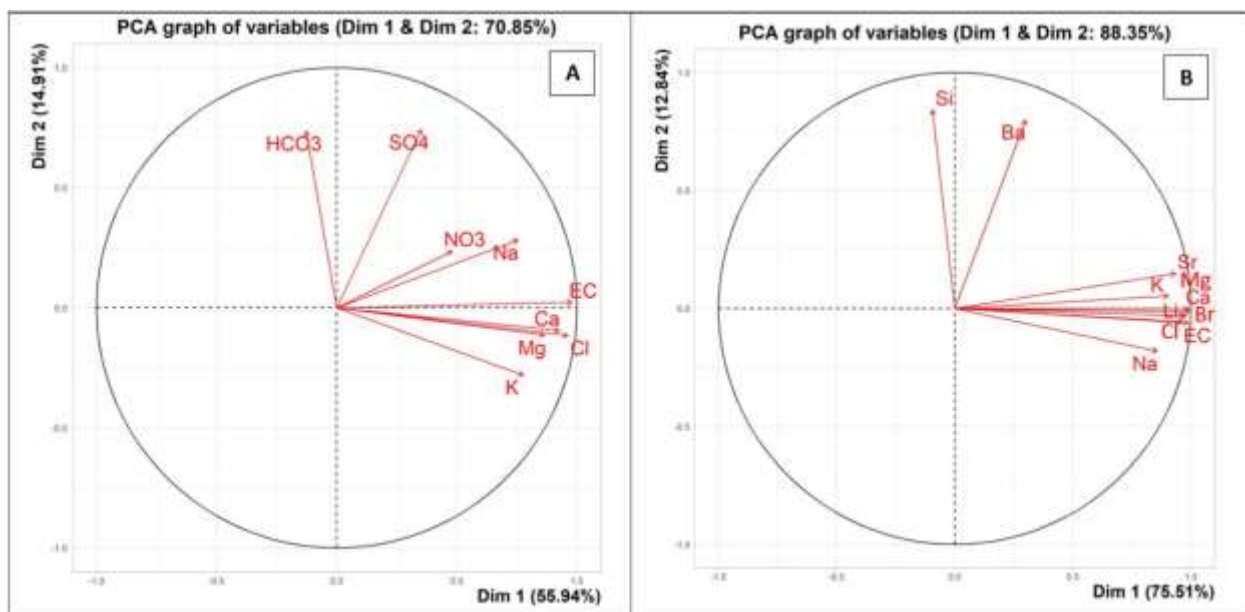


Fig.10

ACCEPTED MANUSCRIPT